SECURITY CLASSIFICATION OF THIS PAGE

FILE COPY

(2)

REPORT DOCUMENTATION PAGE

Form Approved
OMB No. 0704-0188

1a. REPORT SECURITY CLASSIFICATION Unclassified	1b. RESTRICTIVE MARKINGS
AD-A221 517	3. DISTRIBUTION/AVAILABILITY OF REPORT Approved for public release; distribution is unlimited
2b. DECLASSIFICATION/DOWNGRADING SCHEDULE	
4. PERFORMING ORGANIZATION REPORT NUMBER(S)	5. MONITORING ORGANIZATION REPORT NUMBER(S) AFOSR-TR- 90-0446
6a. NAME OF PERFORMING ORGANIZATION Florida Atlantic University 6b. OFFICE SYMBOL (If applicable)	7a. NAME OF MONITORING ORGANIZATION AFOSR/NA
6c. ADDRESS (City, State, and ZIP Code) P.O. Box 3091 Boca Raton, FL 33431-0991	7b. ADDRESS (City, State, and ZIP Code) Building 410, Bolling AFB DC 20332-6448
8a. NAME OF FUNDING/SPONSORING ORGANIZATION AFOSR 8b. OFFICE SYMBOL (If applicable) NA	9. PROCUREMENT INSTRUMENT IDENTIFICATION NUMBER AFOSR-88-0005
8c. ADDRESS (City, State, and ZIP Code) Building 410, Bolling AFB, DC 20332-6448	10. SOURCE OF FUNDING NUMBERS PROGRAM ELEMENT NO. 61102F; PROJECT NO. 2302; TASK NO B1; WORK UNIT ACCESSION NO.

11. TITLE (Include Security Classification)
(U) STOCHASTIC STRUCTURAL DYNAMICS FOR AEROSPACE APPLICATIONS

12. PERSONAL AUTHOR(S) LIN, Y. K.

13a. TYPE OF REPORT	13b. TIME COVERED	14. DATE OF REPORT (Year, Month, Day)	15. PAGE COUNT
final	FROM 11/1/87 TO 12/30/89	3/15/90	92

16. SUPPLEMENTARY NOTATION

17. COSATI CODES			18. SUBJECT TERMS (Continue on reverse if necessary and identify by block number)
FIELD	GROUP	SUB-GROUP	Space Structures, Structural Network, Periodic Structures, Vibration Localization, Nonlinear Random Vibration

19. ABSTRACT (Continue on reverse if necessary and identify by block number)

Three technical areas are addressed: (1) A new general theory is developed to predict the response of a truss-type space structure under arbitrary loading using the concept of wave propagation and scattering in piece-wise periodic structures. (2) The effects of random imperfection (or disorder) are taken into account based on assumed spatial ergodicity property of the imperfect periodic truss units. The random disorder has the tendency to inhibit wave propagation, quantified by a localization factor. A scheme is devised to permit successive improvement of accuracy in the compation of localization factor, making it applicable to all practical cases regardless of the relative measures between disorder and the internal coupling. (3) New exact and approximate solution techniques are developed for nonlinear dynamical systems under random excitation. The exact solution technique is based on separation of probability flow into the potential flow and the circulatory flow. Approximate solution is obtained under a statistical criterion that the average dissipation energy remains the same for the original system and a substituting system which is exactly solvable.

20. DISTRIBUTION/AVAILABILITY OF ABSTRACT	21. ABSTRACT SECURITY CLASSIFICATION
☒ UNCLASSIFIED/UNLIMITED ☒ SAME AS RPT. ☒ DTIC USERS	UNCLASSIFIED
22a. NAME OF RESPONSIBLE INDIVIDUAL Dr. Spencer Wu	22b. TELEPHONE (Include Area Code) (202) 767-6962 22c. OFFICE SYMBOL NM

DD Form 1473, JUN 86 Previous editions are obsolete. SECURITY CLASSIFICATION OF THIS PAGE

TABLE OF CONTENTS

TABLE OF CONTENTS - Continued

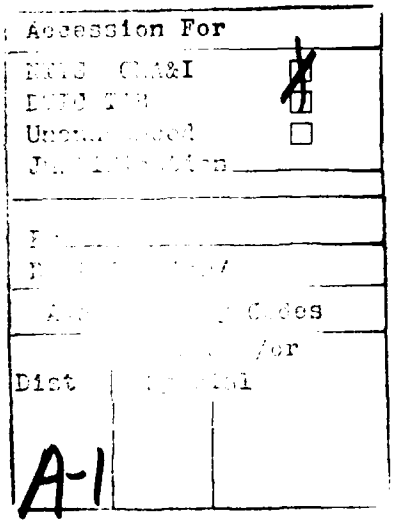

OBJECTIVES OF THE RESEARCH PROGRAM

The main emphasis of the research program is placed on the dynamical performance of truss-type space structures, with the following broad objectives:

(1) Develop a basic theory capable of perdicting accurately the response of a truss-type space structure under arbitrary loading, without making the usual sweeping approximation in which actual truss networks are replaced by Timoshenko beam elements or other continuum elements in the analysis.

(2) Evaluate the effects of random variations in material and geometrical properties in the truss-network construction.

(3) Identify nonlinearities in aerospace strucutural systems and develop new exact and approximate solution techniques for such problems.

DETERMINISTIC ANALYSIS OF TRUSS-TYPE STRUCTURAL NETWORK

Truss-type networks are often used in space-structure designs. Their configurations are generally complex, and a large number of degrees of freedom is required to adequately describe their responses to dynamic excitations. The application of an all-encompassing finite element analysis can be expensive in computer time. In many cases, it may also lead to inaccurate results since some of the natural frequencies may be very close to each other. One way to alleviate this predicament is to substitute the original truss-type network by an equivalent network of Timoshenko-beam elements (e.g. references [1,2]). However, much detailed information is lost in the process which may be important for certain missions of the structure or important in the design of control systems for the structure.

Recognizing the fact that a typical truss network of a space structure consists only of a few sizes of truss units which are connected end-to-end to form piece-wise periodic arrays, recent advances in the field of periodic

structures (e.g. references [4-12]) can be utilized to advantage. The present analysis is based on the concept of wave propagation in periodic structures [4], modified to account for wave scattering when a periodic pattern is distrupted. The finite element or some other conventional formulations may be used to model a single truss unit, transfer matrices are used to relate the state vectors of structural response from unit to unit, and state vectors are converted to wave vectors in order that computation can follow the direction of wave propagation to avoid numerical instability in the computation. The general approach is similar to that adopted by von Flotow [13] who substituted the truss network by Timoshenko-beam network, and by Signorell and von Flotow [14] who were concerned with wave-passage frequency bands, wave modes, and power flow in a purely periodic truss beam. A combined finite element and transfer matrix approach was first proposed by McDaniel and Eversole [15]. The retention of truss unit and the inclusion of piece-wise periodic patterns and structural damping in the analysis do add considerable complications; however, the rewards are more accurate results, and broader applicability.

1. MULTI-CHANNEL WAVE GUIDES

Any identifiable structural element may be viewed as a waveguide, in the sense that disturbances at one location can be transmitted to another. Consider a typical truss unit in a space structure, which has an exterior shape of a right parallelepiped, with eight exterior corners. If the generalized displacements and the associated generalized forces at the four corners on one end of the unit are specified, then the generalized displacements and the associated generalized forces at the four corners on the other end can be determined. Since each corner is capable of six degrees of freedom, three in translation and three in rotation, such a unit is capable of transmitting 24

types of wave motions if the structural members in the unit are rigidly connected at the corners. In the terminology of wave mechanics, it is a 24-channel waveguide. However, if the structural members are pinned at the corners, then the rotational degrees of freedom cannot be transmitted, and the unit reduces to a 12-channel waveguide.

To be more specific, write an equation in the frequency domain relating the state vectors on the two ends of a truss unit, say unit n (or cell n), as follows

$$\begin{Bmatrix} w_{n+1} \\ f_{n+1} \end{Bmatrix} = [T(n)] \begin{Bmatrix} w_n \\ f_n \end{Bmatrix} \tag{1}$$

where each w is a p-dimensional vector of the complex amplitudes of generalized displacements, each f is a p-dimensional vector of the complex amplitudes of the generalized forces, and T is a 2px2p transfer matrix associated with the nth cell. For a typical truss cell, p=24 or p=12 depending on whether the truss members are clamped or pinned at the corners. Using the transformation

$$\begin{Bmatrix} w_n \\ f_n \end{Bmatrix} = [D(n)] \begin{Bmatrix} \mu_n(n,n+1) \\ \mu_n(n+1,n) \end{Bmatrix} \tag{2a}$$

$$\begin{Bmatrix} w_{n+1} \\ f_{n+1} \end{Bmatrix} = [D(n)] \begin{Bmatrix} \mu_{n+1}(n,n+1) \\ \mu_{n+1}(n+1,n) \end{Bmatrix} \tag{2b}$$

where columns in [D(n)] are the eigenvectors of [T(n)] arranged according to an ascending order of the magnitudes of the eigenvalues, equation (1) is replaced by [3]

$$\begin{Bmatrix} \mu_{n+1}(n,n+1) \\ \mu_{n+1}(n+1,n) \end{Bmatrix} = \begin{bmatrix} \Lambda & 0 \\ 0 & \Lambda^{-1} \end{bmatrix} \begin{Bmatrix} \mu_n(n,n+1) \\ \mu_n(n+1,n) \end{Bmatrix} \tag{3}$$

in which Λ is a diagonal matrix of the first p eigenvalues. When deriving equation (3) use is made of the fact that the eigenvalues of a transfer matrix

are reciprocal pairs. Since damping normally exists in a physical system, the magnitude of each eigenvalue in Λ is smaller than one, and each in Λ^{-1} is greater than one. This implies that $\mu_n(n,n+1)$ in the first row of equation (3) represents a wave vector transmitted through cell n, and emerges as $\mu_{n+1}(n,n+1)$. The eigenvalues in Λ account for both reduction of magnitudes and change of phases in the transmission process. In the second row of equation (3), it is the wave vector $\mu_{n+1}(n+1,n)$ which is transmitted through cell n and emerges to become $\mu_n(n+1,n)$. The choice of the subscript and the order of the arguments in denoting a wave vector μ can now be explained. For example, $\mu_n(n,n+1)$ represents a wave vector at location n which is propagated from n to n+1, etc. The cell plays the role of a p-channel waveguide.

Obviously, two p-channel waveguides connected end-to-end is also a p-channel waveguide. Consider, for example, two connected cells, and write the transfer relationship for the state vectors as follows:

$$\begin{Bmatrix} w_{n+2} \\ f_{n+2} \end{Bmatrix} = [T(n+1)][T(n)] \begin{Bmatrix} w_n \\ f_n \end{Bmatrix} \tag{4}$$

It follows upon transformation into wave vectors

$$\begin{Bmatrix} \mu_{n+2}(n,n+2) \\ \mu_{n+2}(n+2,n) \end{Bmatrix} = [Q(n+2,n)] \begin{Bmatrix} \mu_n(n,n+2) \\ \mu_n(n+2,n) \end{Bmatrix} \tag{5}$$

where

$$[Q(n+2,n)] = [D(n+1)]^{-1}[T(n+1)][T(n)][D(n)] \tag{6}$$

Now $[Q(n+2,n)]$ is generally not a diagonal matrix, unless $[T(n+1)]=[T(n)]$, namely, unless cells n and n+1 are identical. It implies that $\mu_{n+2}(n,n+2)$ does not result completely from the transmitted portion of $\mu_n(n,n+2)$.

2. WAVE SCATTERING MATRICES

For an arbitrary array of connected cells, equation (5) is generalized to

$$\begin{Bmatrix} \mu_m(m,n) \\ \mu_m(n,m) \end{Bmatrix} = [Q(n,m)] \begin{Bmatrix} \mu_n(m,n) \\ \mu_n(n,m) \end{Bmatrix} \tag{7}$$

These wave vectors are shown schematically in figure 1. With respect to this waveguide, $\mu_m(m,n)$ and $\mu_n(n,m)$ may be treated as incoming wave vectors whereas $\mu_m(n,m)$ and $\mu_n(m,n)$ treated as outgoing wave vectors. These two types of wave vectors can easily be recognized from their notations. A wave vector is incoming if the subscript and the first argument are the same; it is outgoing if the subscript and the second argument are the same.

Recast equation (7) in a form indicative of an input-output relationship as follows:

$$\begin{Bmatrix} \mu_m(n,m) \\ \mu_n(m,n) \end{Bmatrix} = [S(n,m)] \begin{Bmatrix} \mu_m(m,n) \\ \mu_n(n,m) \end{Bmatrix} \tag{8}$$

where

$$[S(n,m)] = \begin{bmatrix} R(m,n) & T(n,m) \\ T(m,n) & R(n,m) \end{bmatrix} \tag{9}$$

It can be shown that

$$R(m,n) = - [Q_{22}(n,m)]^{-1} Q_{21}(n,m) \tag{10a}$$

$$T(m,n) = Q_{11}(n,m) - Q_{12}(n,m)[Q_{22}(n,m)]^{-1}Q_{21}(n,m) \tag{10b}$$

$$R(n,m) = Q_{12}(n,m) [Q_{22}(n,m)]^{-1} \tag{10c}$$

$$T(n,m) = [Q_{22}(n,m)]^{-1} \tag{10d}$$

where $Q_{ij}(n,m)$ are sub-matrices of $Q(n,m)$ in equation (7). The doubly argumented T and R matrices in equation (9) are called transmission and reflection matrices, respectively. The first argument in the parentheses denoting these matrices indicates the location of an incoming wave vector to be transmitted or reflected. For example, R(m,n) indicates a reflection response

to an incoming wave vector at m, and T(n,m) indicates a transmission response to an incoming wave vector at n. Moreover, the two arguments for example, (m,n) refer to a waveguide extending between m and n, and their order indicates that the incoming wave is in the direction of m to n. Matrix S in equation (8), composed of these transmission and reflection sub-matrices, is called the wave scattering matrix.

It is of interest to point out that an array of cells may contain several sections, each of which is composed of one type of periodic units. Thus, the entire array is a piece-wise periodic structure. The scattering matrix for each section is easy to construct since their transmission matrices are of the form of Λ^j where j is the number of the periodic units in the section, and their reflection matrices are null. The scattering matrix for the interface between two different periodic sections can be determined from a wave-vector transfer matrix Q of the form

$$Q = [D(j+1)]^{-1}[D(j)] \tag{11}$$

according to the rule given by equations (10a-d).

If a waveguide is terminated at a boundary where either the force components are zero (a free boundary) or the displacement components are zero (a clamped boundary), then such a boundary can also be treated as an interface between the end of the waveguide and a fictitious station beyond the waveguide. For instance, let n be a free boundary such that $F_n = 0$. We may write

$$\begin{Bmatrix} w_n \\ 0 \end{Bmatrix} = [D(n)] \begin{Bmatrix} \mu_n(n, F_n) \\ \mu_n(F_n,n) \end{Bmatrix} = \begin{bmatrix} M_n(n,F_n) & M_n(F_n,n) \\ N_n(n,F_n) & N_n(F_n,n) \end{bmatrix} \begin{Bmatrix} \mu_n(n,F_n) \\ \mu_n(F_n,n) \end{Bmatrix} \tag{12}$$

where F_n indicates a fictitious station next to n but outside the waveguide, and where the M_n and N_n are sub-matrices of D(n), which play the roles of converting the outgoing waves $\mu_n(n,F_n)$ and incoming waves $\mu_n(F_n,n)$ into displacements and forces, respectively [8]. From the second row of equation (12),

$$\mu_n(F_n,n) = - [N_n(F_n,n)]^{-1} N_n(n,F_n)\mu_n(n,F_n) \tag{13}$$

Now, the interface between n and F_n may be characterized by a scattering matrix, namely,

$$\begin{Bmatrix} \mu_n(F_n,n) \\ \mu_{F_n}(n,F_n) \end{Bmatrix} = [S(F_n,n)] \begin{Bmatrix} \mu_n(n,F_n) \\ \mu_{F_n}(F_n,n) \end{Bmatrix}$$

$$= \begin{bmatrix} R(n,F_n) & T(F_n,n) \\ T(n,F_n) & R(F_n,n) \end{bmatrix} \begin{Bmatrix} \mu_n(n,F_n) \\ \mu_{F_n}(F_n,n) \end{Bmatrix} \tag{14}$$

However, neither incoming nor outgoing waves exist beyond F_n, we also have $\mu_{F_n}(F_n,n) = \mu_{F_n}(n,F_n) = 0$. It follows that $T(n,F_n) = 0$, and

$$R(n,F_n) = - [N_n(F_n,n)]^{-1} N_n(n,F_n) \tag{15}$$

Matrices $T(F_n,n)$ and $R(F_n,n)$ can be arbitrary, but they are not needed in our calculation.

A clamped boundary where the displacement components must vanish can be treated similarly. Let C_n be a fictitious station next to a clamped boundary n. It can be shown that at the boundary, the transmission matrix $T(n,C_n) = 0$ and the reflection matrix

$$R(n,C_n) = - [M_n(C_n,n)]^{-1} M_n(n,C_n) \tag{16}$$

the concept can further be generalized to the case in which any p components of a 2p state vector must vanish at the boundary. If the vanishing components are of a mixed type, including some force components and some displacement components, it will be necessary to re-arrange the state vector such that the vanishing components are grouped in either the lower half or the upper half. The rows in the M and N matrices must also be rearranged accordingly. The reflection matrix then can be obtained in a similar manner. In what follows, such boundaries are referred to as bounded ends.

Finally, the scattering matrix for a chain of waveguides and interfaces can be constructed sequentially using the composition rule [3]

$$R(i,k) = R(i,j) + T(j,i)\, R(j,k)\, [I-R(j,i)\, R(j,k)]^{-1} \tag{17a}$$

$$T(i,k) = T(j,k)\, [I-R(j,i)\, R(j,k)]^{-1}\, T(i,j) \tag{17b}$$

where station j is between stations i and k. It is also clear from the above discussion that wave reflections in a piece-wise periodic waveguide occur only at the interfaces and boundaries where changes of periodic patterns take place.

Computationally, the use of scattering matrices in the formulation has a distinct advantage; it directs the calculation in the directions of wave propagation and ensures numerical stability. Since damping exists in a structure, the amplitude of a wave motion decreases as it propagates. However, if a portion of computation proceeds in the direction opposite to that of wave propagation, then numerical errors may grow and the results can become meaningless, which is likely to occur when the path of propagation is long.

The dynamic behavior of a junction, where two or more wave guides meet, can also be characterized by a scattering matrix. Figure 2 shows a junction, labeled junction A and possessing of several ports, each of which represent an interface with a waveguide. Each interface is identified by a number; e.g. number j shown in the figure. Then, according to the convention adopted earlier, $\mu_j(A,j)$ is an outgoing wave vector and $\mu_j(j,A)$ is an incoming wave vector with respect to junction A.

A governing equation for junction A can be formulated using any suitable method of structural dynamics, e.g., a finite-element procedure,

$$[P] \begin{Bmatrix} w(1) \\ \vdots \\ w(m) \end{Bmatrix} = \begin{Bmatrix} f(1) \\ \vdots \\ f(m) \end{Bmatrix} \tag{18}$$

where [P] is an impedance matrix, each pair of w(j) and f(j) are displacement and force vectors, respectively at interface j and j=1,2,...,m. The state vector at the jth interface can be transformed into wave vectors by

$$\begin{Bmatrix} w(j) \\ f(j) \end{Bmatrix} = [D(j)] \begin{Bmatrix} \mu_j(A,j) \\ \mu_j(j,A) \end{Bmatrix} = \begin{bmatrix} M_j(A,j) & M_j(j,A) \\ N_j(A,j) & N_j(j,A) \end{bmatrix} \begin{Bmatrix} \mu_j(A,j) \\ \mu_j(j,A) \end{Bmatrix}, \quad j=1,\ldots,m, \tag{19}$$

where [D(j)] is constructed from the eigenvectors of the transfer matrix associated with the cell belonging to the waveguide next to j. Again the M_j and N_j submatrices account for the contributions of wave vectors toward displacements and forces, respectively. Substituting (19) into (18) yields

$$\begin{Bmatrix} \mu_1(A,1) \\ \vdots \\ \mu_m(A,m) \end{Bmatrix} = [S] \begin{Bmatrix} \mu_1(1,A) \\ \vdots \\ \mu_m(m,A) \end{Bmatrix} \tag{20}$$

where [S] is the required scattering matrix for junction A, and is given by

$$[S] = \left([P] \begin{bmatrix} M_1(A,1) & & 0 \\ & \ddots & \\ 0 & & M_m(A,m) \end{bmatrix} - \begin{bmatrix} N_1(A,1) & & 0 \\ & \ddots & \\ 0 & & N_m(A,m) \end{bmatrix}\right)^{-1}$$

$$\times \left(\begin{bmatrix} N_1(1,A) & & 0 \\ & \ddots & \\ 0 & & N_m(m,A) \end{bmatrix} - [P] \begin{bmatrix} M_1(1,A) & & 0 \\ & \ddots & \\ 0 & & M_m(m,A) \end{bmatrix} \right) \tag{21}$$

In this scattering matrix, a total of m square submatrices along the diagonal are reflection matrices, reversing incoming waves back to the same waveguides. The remaining m(m-1) submatrices are transmission matrices redirecting incoming waves at one port to the others. In the special case of m=2, a junction reduces to a waveguide, and equation (20) reduces to equation (8).

3. A WAVEGUIDE SUBJECT TO AN EXCITATION

Figure 3 illustrates a waveguide subject to an excitation at j which is the interface between cells j-1 and j. The excitation, denoted as a source vector $\{w_S, f_S\}$, causes a discontinuity in the wave vector at the interface, given by

$$\begin{Bmatrix} \mu_{j+}(j-,j+) \\ \mu_{j+}(j+,j-) \end{Bmatrix} - [Q(j+,j-)] \begin{Bmatrix} \mu_{j-}(j-,j+) \\ \mu_{j-}(j+,j-) \end{Bmatrix} = \begin{bmatrix} M_j(j-,j+) & M_j(j-,j+) \\ N_j(j-,j+) & N_j(j-,j+) \end{bmatrix}^{-1} \begin{Bmatrix} w_S \\ f_S \end{Bmatrix} = \begin{Bmatrix} \sum_1 \\ \sum_2 \end{Bmatrix} \quad (22)$$

where j- and j+ are the two sides of interface j, and $Q(j+,j-)=[D(j)]^{-1}[D(j-1)]$. In general, only one-half of the elements in the source vector are non-zero. Equation (22) may be re-arranged to read

$$\begin{Bmatrix} \mu_{j-}(j+,j-) \\ \mu_{j+}(j-,j+) \end{Bmatrix} = [S] \begin{Bmatrix} \mu_{j-}(j-,j+) \\ \mu_{j+}(j+,j-) \end{Bmatrix} + \begin{bmatrix} 0 & -T(j+,j-) \\ I & -R(j+,j-) \end{bmatrix} \begin{Bmatrix} \sum_2 \\ \sum_1 \end{Bmatrix} \quad (23)$$

in which [S] is a scattering matrix that can be contructed using the elements of matrix Q(j+, j-).

Now, treating the two sections m to j- and j+ to n, as two separate waveguides, equation (23) may be rewritten as follows:

$$\begin{Bmatrix} \mu_{j-}(j+,j-) \\ \mu_{j+}(j-,j+) \end{Bmatrix} = \left(I - [S] \begin{bmatrix} R(m,j-) & 0 \\ 0 & R(j+,n) \end{bmatrix}\right)^{-1} x$$

$$\left([S] \begin{bmatrix} T(j-,m) & 0 \\ 0 & T(n,j+) \end{bmatrix} \begin{Bmatrix} \mu_m(m,j) \\ \mu_n(n,j) \end{Bmatrix} + \begin{bmatrix} 0 & -T(j+,j-) \\ I & -R(j+,j-) \end{bmatrix} \begin{Bmatrix} \sum_1 \\ \sum_2 \end{Bmatrix}\right) \quad (24)$$

Noticing the relationships,

$$\mu_m(j,m) = R(m,j-)\mu_m(m,j) + T(j-,m)\mu_{j-}(j+,j-) \quad (25)$$

$$\mu_n(j,n) = R(n,j+)\mu_n(n,j) + T(j+,n)\mu_{j+}(j-,j+) \quad (26)$$

$\mu_{j+}(j-,j+)$ and $\mu_{j-}(j+,j-)$ can be eliminated by using equation (24), arriving at

$$\begin{Bmatrix} \mu_m(n,m) \\ \mu_n(m,n) \end{Bmatrix} = \begin{bmatrix} R(m,n) & T(n,m) \\ T(m,n) & R(n,m) \end{bmatrix} \begin{Bmatrix} \mu_m(m,n) \\ \mu_n(n,m) \end{Bmatrix}$$

$$+ \begin{bmatrix} T(j-,m) & 0 \\ 0 & T(j+,n) \end{bmatrix} \left[I - [S] \begin{bmatrix} R(j-,m) & 0 \\ 0 & R(j+,n) \end{bmatrix} \right]^{-1} \begin{bmatrix} 0 & -T(j+,j-) \\ I & -R(j-,j+) \end{bmatrix} \begin{Bmatrix} \sum_1 \\ \sum_2 \end{Bmatrix} \quad (27)$$

in which the identities $\mu_m(j,m)=\mu_m(n,m)$, etc. have been used. This equation shows how the relation between the incoming and the outgoing waves is changed due to the presence of external excitation.

Equation (27) is written in a form indicative of the adopted computational scheme in which the outgoing waves are treated as unknowns and solved in terms of the external excitations and the incoming waves. In actuality, the incoming waves are also unknowns, and two additional equations are needed for a complete solution. If both ends of a waveguide are bounded, then the required two equations can be obtained in the form of equation (13). If one end is connected to another waveguide, then the incoming waves for one waveguide are exactly the outgoing waves for the connecting waveguide. Thus, only the outgoing waves need be treated as unknowns and numerical stability is assured in the computation.

4. STRUCTURAL RESPONSE

The response of a structure at a certain location k due to an external excitation at another location j can be formulated most simply by referring to a waveguide which contain k but not j. This arrangement is always possible as can easily be explained with the aid of figure 3. Here k is shown to be between m and j. Then a waveguide extending from m to ℓ, where ℓ is between k and j, will meet such a requirement. Referring to this waveguide, we obtain

$$\begin{Bmatrix} w(k) \\ f(k) \end{Bmatrix} = \begin{bmatrix} M_k(m,k) & M_k(k,m) \\ N_k(m,k) & N_k(k,m) \end{bmatrix} \begin{bmatrix} [I-R(k,m)\ R(k,\ell)]^{-1} & 0 \\ 0 & [I-R(k,\ell)R(k,m)]^{-1} \end{bmatrix}$$

$$x \begin{bmatrix} T(m,k) & R(k,m)T(\ell,k) \\ R(k,\ell)T(m,k) & T(\ell,k) \end{bmatrix} \begin{Bmatrix} \mu_m(m,\ell) \\ \mu_n(\ell,m) \end{Bmatrix} \quad (28)$$

It is of interest to note the following special cases:

4-1. WAVEGUIDE WITH A BOUNDED END AND WITHOUT EXTERNAL EXCITATION

In this case, there is no incoming wave at the bounded end. For example, if m is a free end, then $\mu_{F_m}(F_m,\ell)=0$. The displacement response at k can be obtained from equation (28) as

$$w(k) = [M_k(F_m,k)R(k,F_m) + M_k(k,F_m)][I-R(k,\ell)R(k,F_m)]^{-1} \; T(\ell,k)\mu_n(\ell,k) \quad (29)$$

4-2. CLOSED LOOP

A schematic of a closed loop is shown in figure 4. An external excitation is applied at a cell-to-cell interface, labeled 1. The numbering of other interfaces proceeds clockwise, assuming that an observer is inside the closed loop. The excitation gives rise to a discontinuity

$$\begin{Bmatrix} w_s \\ f_s \end{Bmatrix} = \begin{Bmatrix} w(1+) \\ f(1+) \end{Bmatrix} - \begin{Bmatrix} w(1-) \\ f(1-) \end{Bmatrix} \quad (30)$$

For simplicity, let the two adjoining cells at 1 be identical. Then from equation (22)

$$\begin{Bmatrix} \mu_{1+}(1+,1-) \\ \mu_{1+}(1-,1+) \end{Bmatrix} - \begin{Bmatrix} \mu_{1-}(1+,1-) \\ \mu_{1-}(1-,1+) \end{Bmatrix} = \begin{bmatrix} M_1(1+,1-) & M_1(1-,1+) \\ N_1(1+,1-) & N_1(1-,1+) \end{bmatrix}^{-1} \begin{Bmatrix} w_s \\ f_s \end{Bmatrix} = \begin{Bmatrix} \sum_1 \\ \sum_2 \end{Bmatrix} \quad (31)$$

To render equation (28) applicable, the closed loop is treated as a waveguide with boundaries at 1+ and 1-. From such a point of view, the waveguide is without an external excitation. Clearly then

$$\begin{Bmatrix} \mu_{1+}(1-,1+) \\ \mu_{1-}(1+,1-) \end{Bmatrix} = \begin{bmatrix} R(1+,1-) & T(1-,1+) \\ T(1+,1-) & R(1-,1+) \end{bmatrix} \begin{Bmatrix} \mu_{1+}(1+,1-) \\ \mu_{1-}(1-,1+) \end{Bmatrix} \quad (32)$$

Substituting (32) into (31) and re-arranging,

$$\begin{Bmatrix} \mu_{1+}(1+,1-) \\ \mu_{1-}(1-,1+) \end{Bmatrix} = \begin{bmatrix} \sigma_{11} & 0 \\ 0 & \sigma_{22} \end{bmatrix} \begin{bmatrix} I & -R(1-,1+) \\ R(1+,1-) & I \end{bmatrix} \begin{Bmatrix} \sum_1 \\ \sum_2 \end{Bmatrix} \tag{33}$$

where

$$\sigma_{11}^{-1} = I - T(1-,1+) - R(1+,1-)[I-T(1+,1-)]^{-1}R(1-,1+) \tag{34a}$$

$$\sigma_{22}^{-1} = I - T(1+,1-) - R(1-,1+)[I-T(1-,1+)]^{-1}R(1+,1-) \tag{34b}$$

Equation (33) describes the two incoming wave vectors at the two ends of the waveguide extending clockwise from 1+ to 1-. Thus, the structural response can be determined using equation (28). For example, the displacement response at k is given by

$$\begin{aligned} w(k) = {} & [M_k(1,k)\ R(k,1+) + M_k(k,1)][I-R(k,1-)R(k,1+)]^{-1}\ T(1-,k)\mu_{1-}(1-,1+) \\ & + [M_k(1,k) + M_k(k,1)R(k,1-)][I-R(k,1+)R(k,1-)]^{-1}\ T(1+,k)\mu_{1+}(1+,1-) \\ & \qquad k = 1+,\ 2,\ \ldots,\ n,\ 1- \end{aligned} \tag{35}$$

5. AN ELIMINATION PROCEDURE

The structural response discussed in Section 5 has been expressed in terms of a one-dimensional waveguide. To obtain the response for more complicated structures, it is conceptionally convenient to convert such structures to equivalent one-dimensional waveguides. This can be accomplished by use of an elimination procedure which will be explained below for various cases of increasing complexity.

5.1 A WAVEGUIDE WITH AN ADJOINING JUNCTION ON ONE END AND BOUNDED ON THE OTHER

Shown in figure 5 is a waveguide which interfaces with an m-port junction A on its left end m and is bounded on its right with a free end F_n. Noticing that

$\mu_m(A,m)=\mu_m(m,F_n)$ and $\mu_m(m,A)=\mu_m(F_n,m)$, we obtain from substituting (13) into (20),

$$\begin{Bmatrix} \mu_1(A,1) \\ \vdots \\ \mu_{m-1}(A,m-1) \\ \mu_m(A,m) \end{Bmatrix} = [S] \begin{bmatrix} I & & & \\ & \ddots & & 0 \\ & & I & \\ 0 & & & R(m,F_n) \end{bmatrix} \begin{Bmatrix} \mu_1(1,A) \\ \vdots \\ \mu_{m-1}(m-1,A) \\ \mu_m(A,m) \end{Bmatrix} \tag{36}$$

which is valid when no external excitation is present on the waveguide. Equation (36) can be simplified to

$$\begin{Bmatrix} \mu_1(A,1) \\ \vdots \\ u_{m-1}(a,m-1) \\ 0 \end{Bmatrix} = \begin{bmatrix} U_{11} & U_{12} \\ \hline U_{21} & \bar{U}_{22} \end{bmatrix} \begin{Bmatrix} \mu_1(1,A) \\ \vdots \\ \mu_{m-1}(m-1,A) \\ \mu_m(A,m) \end{Bmatrix} \tag{37}$$

where U_{ij} are submatrices of the product of the two square matrices on the left hand side of equation (36) and $\bar{U}_{22} = U_{22} - I$. Eliminating wave vector $\mu_m(A,m)$ from equation (37), we obtain

$$\begin{Bmatrix} \mu_1(A,1) \\ \vdots \\ \mu_{m-1}(A,m-1) \end{Bmatrix} = [S_{m-1}] \begin{Bmatrix} \mu_1(1,A) \\ \vdots \\ \mu_{m-1}(m-1,A) \end{Bmatrix} \tag{38}$$

in which $S_{m-1} = U_{11} - U_{12}\,\bar{U}_{22}^{-1}\,U_{21}$. Equation (38) suggests that S_{m-1} may be considered as a scattering matrix for a new junction with m-1 ports.

If an external excitation is applied on a bounded waveguide, then equation (27) must be employed before implementing the elimination procedure, in which case a nonhomogeneous term due to the excitation will appear in equation (38). For the case of several bounded waveguides intersecting at a junction, the same elimination procedure can be applied sequentially.

5.2 A WAVEGUIDE WITH AN ADJOINING JUNCTION ON EACH END

As shown in figure 6, a waveguide is connected to an m-port junction A at its left end m, and connected to a k + 1-port junction B at its right end n. External excitations are applied at a station j on the waveguide between m and n. To proceed, we first assemble the scattering relationships for both junctions as follows

$$\begin{matrix} \mu_i(A,1) \\ \vdots \\ \{\mu_m(A,m)\} \\ \mu_n(B,n) \\ \vdots \\ \mu_{n+k}(B,n+k) \end{matrix} = \begin{bmatrix} S_A & 0 \\ 0 & S_B \end{bmatrix} \begin{matrix} \mu_i(1,A) \\ \vdots \\ \{\mu_m(m,A)\} \\ \mu_n(R,B) \\ \vdots \\ \mu_{n+k}(n+k,B) \end{matrix} \tag{39}$$

where S_A and S_B are scattering matrices for junctions A and B, respectively. Rearrange equation (39) by moving wave vectors at m and n to the last row to obtain

$$\begin{matrix} \mu_i(A,1) \\ \vdots \\ \{\mu_m(B,n+1)\} \\ \vdots \\ \mu_m(A,m) \\ \mu_n(B,n) \end{matrix} = [S] \begin{matrix} \mu_i(1,A) \\ \vdots \\ \{\mu_{n+i}(n+1,B)\} \\ \vdots \\ \mu_m(m,A) \\ \mu_n(n,B) \end{matrix} \tag{40}$$

Note that the wave vectors at the two ends of a waveguide can be related in the form of equation (27) and that $\mu_m(A,m)=\mu_m(m,n)$, $\mu_m(m,A)=\mu_m(n,m)$, $\mu_n(B,n)=\mu_n(n,m)$ and $\mu_n(n,B)=\mu_n(m,n)$. Substitution of equation (27) into equation (40) yields

$$
\begin{Bmatrix} \mu_1(A,1) \\ \vdots \\ \mu_{m-1}(A,m-1) \\ \mu_{n+1}(B,n+1) \\ \vdots \\ \mu_{n+k}(B,n+k) \\ \mu_m(A,m) \\ \mu_u(B,n) \end{Bmatrix} = [S] \begin{bmatrix} I & & & & & \\ & I & & & & \\ & & \ddots & & & \\ & & & \ddots & & \\ & & & & \ddots & \\ & & & & R(m,n) & T(n,m) \\ & & & & T(m,n) & R(n,m) \end{bmatrix} \begin{Bmatrix} \mu_1(1,A) \\ \vdots \\ \mu_{m-1}(m-1,A) \\ \mu_{n+1}(n,B) \\ \vdots \\ \mu_{n+k}(n+k,B) \\ \mu_m(A,m) \\ \mu_n(B,n) \end{Bmatrix}
$$

$$
+ [S] \begin{Bmatrix} 0 \\ 0 \\ \vdots \\ 0 \\ \Gamma_m \\ \Gamma_n \end{Bmatrix} \tag{41}
$$

where

$$
\begin{Bmatrix} \Gamma_m \\ \Gamma_n \end{Bmatrix} = \begin{bmatrix} T(j-,m) & 0 \\ 0 & T(j+,m) \end{bmatrix} \left[I - \begin{bmatrix} R(j-,j+) & T(j+,j-) \\ T(j-,j+) & R(j+,j-) \end{bmatrix} \begin{bmatrix} R(j-,m) & 0 \\ 0 & R(j+,n) \end{bmatrix} \right]^{-1}
$$

$$
\times \begin{bmatrix} 0 & -T(j+,j-) \\ I & -R(j-,j+ \end{bmatrix} \begin{Bmatrix} \Sigma_1 \\ \Sigma_2 \end{Bmatrix} \tag{42}
$$

Equation (42) implies that when computing structural response at a location outside the waveguide m-n, the effects of the external excitations at j can be accounted for by "equivalent" excitations at stations m and n.

To proceed further, denote

$$
\begin{matrix}
\Sigma(1) & & \\
\cdot & & \\
\cdot & & 0 \\
\cdot & & 0 \\
\Sigma(m-1) & & \cdot \\
\{\Sigma(n+1)\} & = [S] & \{\ \cdot\ \} \\
\cdot & & \cdot \\
\cdot & & \Gamma_m \\
\cdot & & \Gamma_n \\
\Sigma(n+k) & & \\
\Sigma(m) & & \\
\Sigma(n) & &
\end{matrix}
\qquad (43)
$$

Making use of the same elimination procedure as that of Section 6-1, we obtain

$$
\begin{matrix}
\mu_1(A,1) & & \mu_1(1,A) & \Sigma(1) & \\
\cdot & & \cdot & \cdot & \\
\cdot & & \cdot & \cdot & \\
\cdot & & \cdot & \cdot & \\
\mu_{m-1}(A,m-1) & & \mu_{m-1}(m-1,A) & \Sigma(m-1) & \bar{}^{-1}\ \Sigma(m) \\
\{\mu_{m+1}(B,n+1)\} & = [U_{11}-U_{12}\bar{U}_{22}^{-1}U_{21}]\ \{\mu_{n+1}(n+1,B)\} & + \{\Sigma(n+1)\} & - U_{12}\bar{U}_{22}\ \{\quad\} \\
\cdot & & \cdot & \cdot & \Sigma(n) \\
\cdot & & \cdot & \cdot & \\
\cdot & & \cdot & \cdot & \\
\mu_{n+k}(B,n+k) & & \mu_{n+k}(n+k,B) & \Sigma(n+k) &
\end{matrix}
\qquad (44)
$$

in which U_{ij} are the submatrices of the product of the two square matrices on the right hand side of equation (41) and $\bar{U}_{22}=U_{22}-I$. It is of interest to note that although the wave vectors at the two ends of the waveguide do not appear in equation (44), their effects are included in an equivalent new junction with ports 1, 2, ..., m-1 and n+1, ..., n+k. When external excitations are absent equation (44) reduces to a relationship among the scattering waves at these ports.

6. COMPLEX STRUCTURAL NETWORKS

Results obtained in the previous sections can now be applied to complex

structural networks. To illustrate, consider a specific structure shown in figure 7 in which waveguides are represented by solid straight lines and are labeled with circled numbers, and junctions are denoted by capital letters A through F. An excitation is applied on waveguide (2) and the response is to be calculated at a given location on waveguide (1). A number without circle indicates the interface between a port and a waveguide. The reason for assigning numbers (1) and (2) to the two waveguides where the output and the input are located will become obvious in the following development.

First, we assemble the wave vectors at the ports of all junctions and obtain an equation

$$\begin{Bmatrix} \mu\#(A,\#) \\ \mu\#(B,\#) \\ \vdots \\ \mu\#(F,\#) \end{Bmatrix} = \begin{bmatrix} S_A & & & \\ & S_B & & \\ & & \ddots & \\ & & & S_C \end{bmatrix} \begin{Bmatrix} \mu\#(\#,A) \\ \mu\#(\#,B) \\ \vdots \\ \mu\#(\#,F) \end{Bmatrix} \tag{45}$$

where S_A, S_B, ..., and S_F are scattering matrices for junctions A, B, ..., and F, respectively, and where each "#" indicates an interface. It is to be understood that, when representing either incoming or outgoing waves with respect to a multi-port junction, the symbol # ranges over all the ports. For instance, referring to figure 7, $\mu\#(A,\#)$ represents all the outgoing waves from junction A; namely, it is an abbreviation of the vectors $\{\mu_1(A,1)\}$, $\{\mu_8(A,8)\}$, and $\{\mu_{11}(A,11)\}$.

Rearrange the order of wave vectors in equation (45) in the numerical order of the interfaces

$$\begin{Bmatrix} \mu_1(*,1) \\ \vdots \\ \mu_{20}(*,20) \end{Bmatrix} = [S] \begin{Bmatrix} \mu_1(1,*) \\ \vdots \\ \mu_{20}(20,*) \end{Bmatrix} \tag{46}$$

where each "*" signifies a particular junction from A to F. The new scattering matrix [S] in equation (46) is of course not a band matrix. Now, for the

waveguides (3) to (11), the scattering relationship may be written as

$$\mu_{\#}(\#,*) = [S_k]\mu_{\#}(*,\#) \qquad k = 3, \ldots, 11 \tag{47}$$

in which each "#" represents one particular end of the kth waveguide and "*" indicates the junction to which the kth waveguide is connected. Moreover, as shown in figure 7, (3) and (11) are bounded on one end. Thus, S_3 and S_{11} are reflection matrices of order pxp instead of 2px2p. Substituting (47) into (46), we obtain

$$\begin{Bmatrix} \mu_1(*,1) \\ \vdots \\ \mu_4(*,4) \\ \mu_5(*,5) \\ \vdots \\ \mu_{20}(*,20) \end{Bmatrix} = [S] \begin{bmatrix} I & & & & 0 \\ & & & & \\ & & & & \\ & & S_3 & & \\ & & & \ddots & \\ 0 & & & & S_{11} \end{bmatrix} \begin{Bmatrix} \mu_1(1,*) \\ \vdots \\ \mu_4(4,*) \\ \mu_5(*,5) \\ \vdots \\ \mu_{20}(*,20) \end{Bmatrix} \tag{48}$$

The same elimination procedure employed before can be applied to eliminate μ_5 through μ_{20} in equation (48), resulting in

$$\begin{Bmatrix} \mu_1(A,1) \\ \mu_2(B,2) \\ \mu_3(D,3) \\ \mu_4(F,4) \end{Bmatrix} = [\bar{S}] \begin{Bmatrix} \mu_1(1,A) \\ \mu_2(2,B) \\ \mu_3(3,D) \\ \mu_4(4,F) \end{Bmatrix} \tag{49}$$

Since the excitation is applied on waveguide (2), the scattering matrix for waveguide (2) can be used to reduce equation (49) to

$$\begin{Bmatrix} \mu_1(A,1) \\ \mu_2(B,2) \end{Bmatrix} = [U_{11} - U_{12}\bar{U}_{22}^{-1}U_{21}] \begin{Bmatrix} \mu_1(1,A) \\ \mu_2(2,B) \end{Bmatrix} + \begin{Bmatrix} \sum(1) \\ \sum(2) \end{Bmatrix} - U_{12}\bar{U}_{22}^{-1} \begin{Bmatrix} \sum(3) \\ \sum(4) \end{Bmatrix} \tag{50}$$

according to equation (44). Equation (50) indicates an input-output relationship for a one-dimentional waveguide which is equivalent to the network containing all the intersections and waveguides (2) through (11). Noticing that

$$\begin{Bmatrix} \mu_1(1,A) \\ \mu_2(2,B) \end{Bmatrix} = [S_1] \begin{Bmatrix} \mu_1(A,1) \\ \mu_2(B,2) \end{Bmatrix} \tag{51}$$

the incoming waves at the two ends of waveguide (1) are

$$\begin{Bmatrix} \mu_1(A,1) \\ \mu_2(B,2) \end{Bmatrix} = [I-[U_{11}-U_{12}\bar{U}_{22}^{-1}U_{21}][S_1]]^{-1} \left[\begin{Bmatrix} \sum(1) \\ \sum(2) \end{Bmatrix} - U_{12}\bar{U}_{22}^{-1} \begin{Bmatrix} \sum(3) \\ \sum(4) \end{Bmatrix}\right] \tag{52}$$

Finally, the response at an arbitrary location on waveguide (1) can be calculated from equation (28).

Notice that a matrix inversion is required when obtaining equation (49) from equation (48). This inversion can be expensive when the number of waveguides is large. Alternatively, instead of assembling all the junctions in the beginning as shown in equation (45), one can carry out the elimination procedure one waveguide at a time, starting with one or two junctions. More junctions are added successively, until the entire process is complete. Such a step-by-step elimination scheme involves inversions of smaller matrices, and requires much less computational efforts. For the specific example shown in figure 7, we can begin with junction F, and eliminate first waveguide (11). Add successively junctions E, D, and C, and eliminate waveguides (10), (9), through (3) one by one.

7. A NUMERICAL EXAMPLE

Numerical calculation has been carried out for a hypothetical space structure shown in figure 8. The global form of the structure has two closed loops, six junctions and two free-ended arrays. The array in the N-S direction shared by the two closed loops consists of 32 cells. Two additional N-S arrays with 32 cells each and four E-W arrays with 41 cells each complete the two closed loops. The free-ended array to the north are composed of 40 cells and

the free-ended array to the south composed of 80 cells. The two cells, each of which is shared by four intersecting arrays are treated as four-port junctions. The four corner cells are treated as two-port junctions.

The construction of a typical cell unit is depicted in figure 9. The two diagonal bars on each face are assumed to be unconnected at the intersection. All bars are of a cross-section area of 5.02×10^{-3} m^2, and are pinned at the corners of the cell; thus, bending moments cannot be developed in the bars. In this case, the structure cannot resist the rotational degrees of freedom at the corners, and only three translational degrees of freedom per corner need be retained in the analysis. Still, for this model structure, the total number of degrees of freedom is over 5000.

The material properties used in the calculation include Young's modulus $E = 69.6 \times 10^9 (1+i\gamma \text{ sgn } \omega)$ N/m^2, where $\gamma = 0.01$, and the mass density $\rho = 3.77 \times 10^3$ kg/m^3.

Referring to figure 8, an excitation in the E-W direction is applied at station j which is at the middle of an N-S array. The corresponding force responses are calculated at two stations: station h and station k. Station k is located at the interface between the 16th and the 17th cells counting from the western end of an E-W array as shown, while station h is at the interface between the 10th and the 11th cells counting from the southern free end of an N-s array.

Shown in figure 10 is the computed magnitude of the frequency response function $H_k(\omega)$ for the vertical shear force response at k. Significant response is found for frequencies as high as 550 rad/s, apparently involving many modes. Thus, the usual assumption of dominant lower modes in a conventional modal analysis can lead to significant errors in this case. Figure 11 shows the corresponding impulse response in the time domain. No response is felt at k

until about 0.0388 seconds when fastest traveling waves arrive. These waves are associated with higher frequencies, and they travel through the shortest path containing 77 cells. The time delay of 0.0388 suggests that the speed of the first arriving wave is about 2000 cells per second. After reaching a maximum at t = 0.048 sec, the response gradually dies down until about 0.666 sec, when the second wave group arrives also through the shortest path. The response is reinforced further by the higher velocity waves propagating through the second shortest path containing 144 cells. The very complicated time-history after 0.095 sec indicates the superposition of waves traveling through different paths at different velocities and scattering at the junctions.

The frequency response and the corresponding impulse response of the induced horizontal shear force at h are shown in figures 12 and 13, respectively. It is interesting to note that in contrast to the case of location k, lower modes with frequencies ranging from 0 to 200 rad/s, now dominate the response. The shortest path from j to h contains 127 cells; thus it takes 0.064 sec for the fastest traveling waves to arrive to the site, as indicated in the impulse response plot.

8. CONCLUDING REMARKS

In the above analysis, attention is focused on structural response at the interfaces of truss units, bypassing detailed motions in the individual bars within each unit. This is in line with the usual treatment of wave propagation in periodic structures [4]. If responses of certain individual bars are of interest, then these bars and perhaps some other surrounding bars must be treated also as waveguides. In such a case, the theory developed herein is still applicable, except for the additional expense in computer time. The need to investigate individual structural members appears quite realistic for civil engineering structures.

9. REFERENCES

1. Noor, A. K., and Anderson, M. S., "Continuum Model for Beam- and Plate Like Lattice Structures," AIAA Journal, Vol. 16, 1978, pp. 1219-1228.

2. Sun, C. T., Kim, B. J. and Bogdanoff," On the Derivation of Equivalent Simple Models for Beam-and Plate-Like Structures in Dynamic Analysis," Proceeding 1981 AIAA Dynamics Specialists Conference, pp. 523-532.

3. Yong, Y., and Lin, Y. K., "Dynamics of Complex Truss-Type Space Structures," Proceedings, AIAA/ASME/ASCE/AHS/ASC 30th Structures, Structural Dynamics and Materials (SDM) Conference, Mobile, Alabama, April 3-5, 1989, pp. 1295-1304.

4. Brillouin, L., Wave Propagation in Periodic Structures, Dover, New York, 1953.

5. Miles, J. W., "Vibration of Beams on Many Supports," Journal of Engineering Mechanics Division, ASCE Vol. 82, EMI, 1953, pp. 1-9.

6. Lin, Y. K., "Free Vibration of Continous Beam on Elastic Supports," Journal of Mechanical Sciences, Vol. 4, 1962, pp. 409-423.

7. Lin, Y. K., and McDaniel, T. J., "Dynamics of Beam-Type Periodic Structures," Journal of Engineering for Industry, Vol. 91, 1969, pp. 1133-1141.

8. Yong, Y., and Lin, Y. K., "Propagation of Decaying Waves in Periodic and Piece-Wise Periodic Structures," Journal of Sound and Vibration, Vol. 129, 1989, pp. 99-118.

9. Mead, D. J., "Free Wave Propagation in Periodically Supported Infinite Beams," Journal of Sound and Vibration, Vol. 11, 1970, pp. 181-197.

10. Mead, D. J., "A General Theory of Harmonic Wave Propagation in Linear Periodic Systems with Multiple Coupling," Journal of Sound and Vibration, Vol. 27, 1973, pp. 235-260.

11. Mead, D. J., "Wave Propagation and Natural Modes in Periodic Systems: I. Mono-Coupled Systems, II. Multi-Coupled systems, With and Without Damping," Journal of Sound and Vibration, Vol. 40, 1975, pp. 1-39.

12. Mead, D. J., and Markus, S., "Coupled Flexural-Longitudinal Wave Motion in Periodic Beam," Journal of Sound and Vibration, Vol. 90, 1983, pp. 1-24.

13. von Flotow, A. H., "Disturbance Propagation in Structural Network," Journal of Sound and Vibration, Vol. 106, 1986, pp. 433-450.

14. Signorell, J., and von Flotow, A. H., "Wave Propagation, Power Flow, and Resonance in a Truss Beam," Journal of Sound and Vibration, Vol. 126, 1988, pp. 127-144.

15. McDaniel, T. J. and Eversole, K. B., "A Combined Finite Element-Transfer Matrix Structural Analysis Method," Jouranl of Sound and Vibration, Vol. 51, 1977, pp. 157-169.

16. Yong, Y. and Lin, Y. K., "Dynamic Response Analysis of Truss-Type Structural Network - A Wave Propagation Approach", to appear.

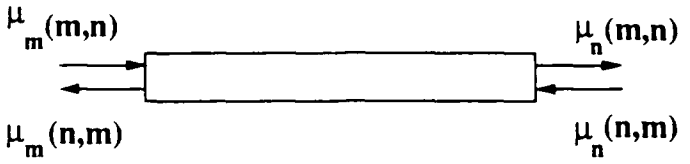

Fig.1 A waveguide with incoming and outgoing waves at the ends.

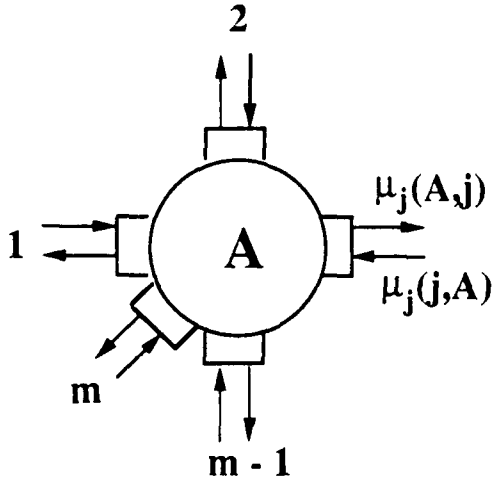

Fig.2 A m-port junction.

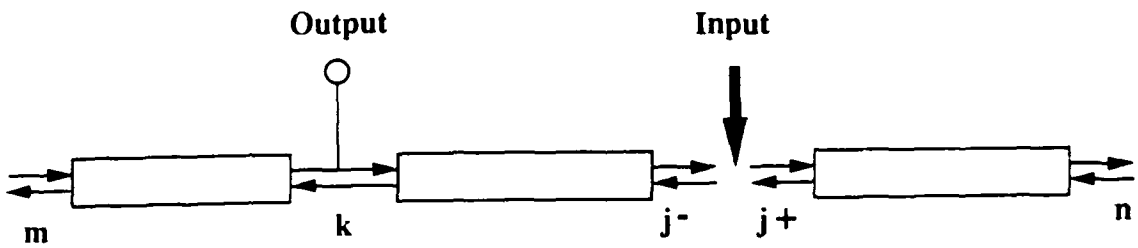

Fig.3 A waveguide subject to an external excitation.

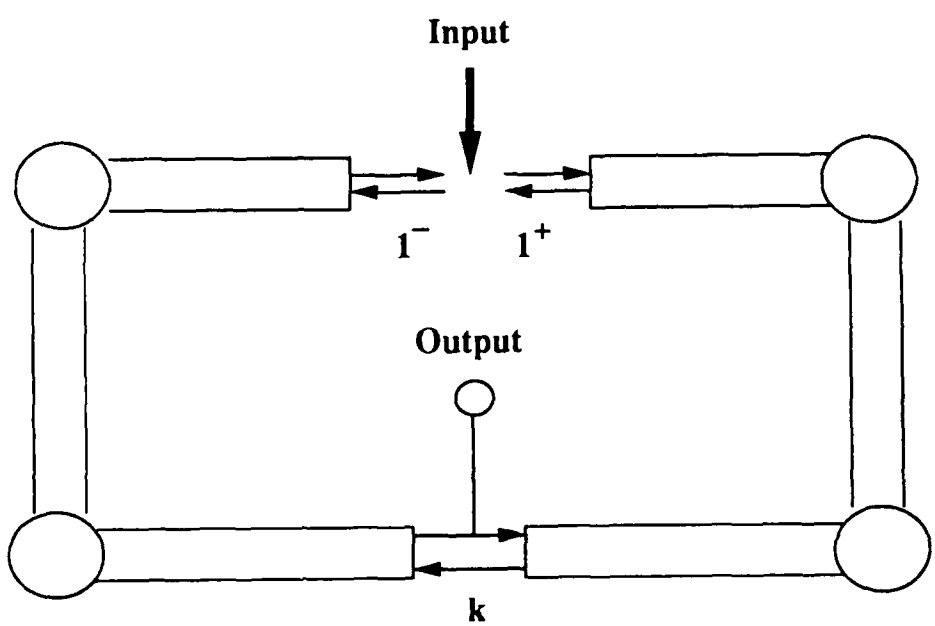

Fig.4 A closed-loop waveguide subject to an external excitation

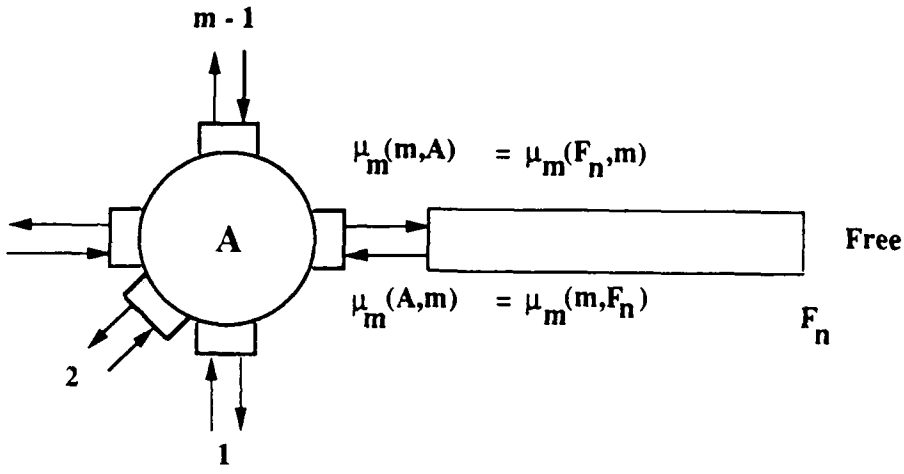

Fig.5 A waveguide with an adjoining junction on one end and bounded on the other end.

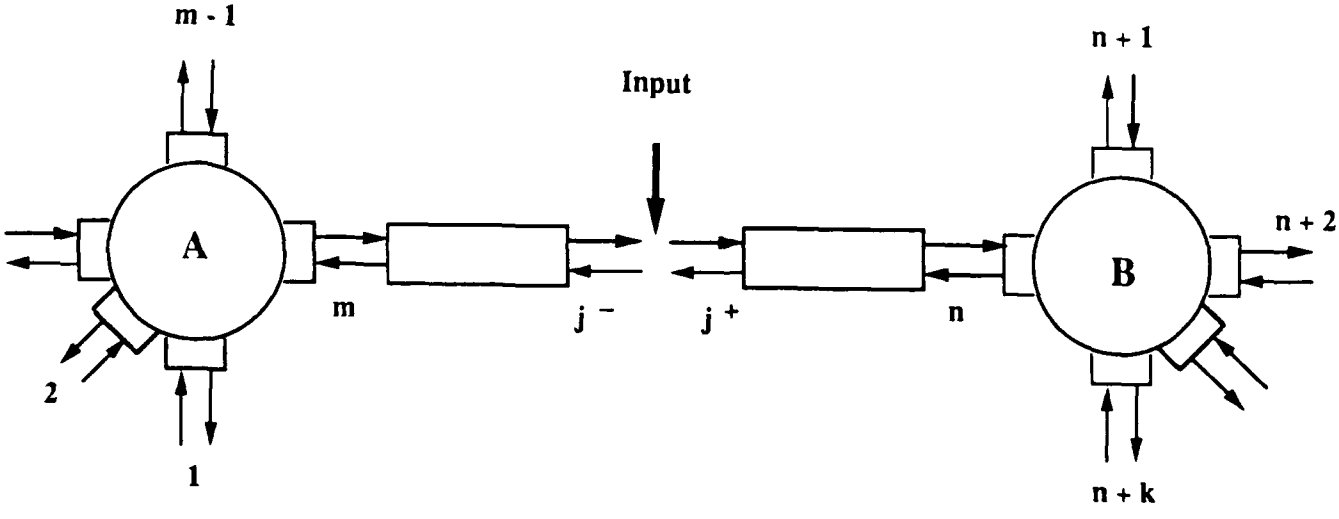

Fig.6 A waveguide with an adjoining junction on each end.

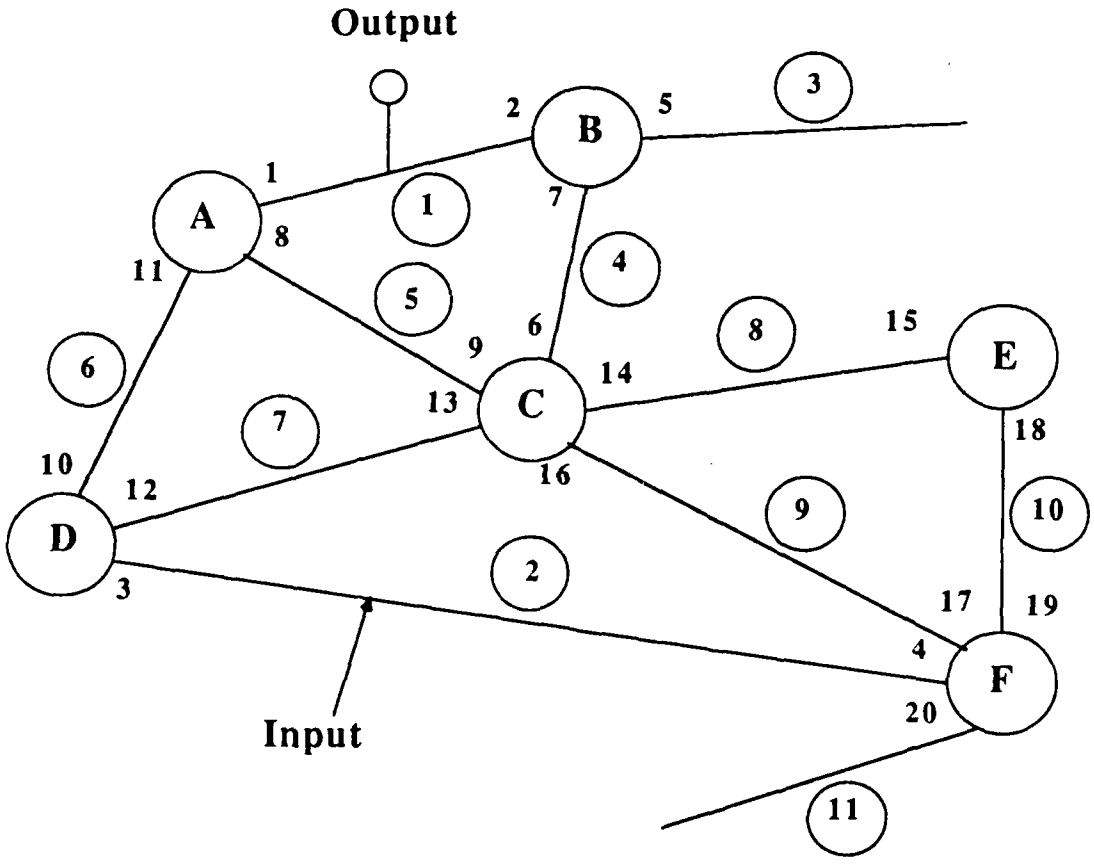

Fig.7 Schematic of an example truss network.

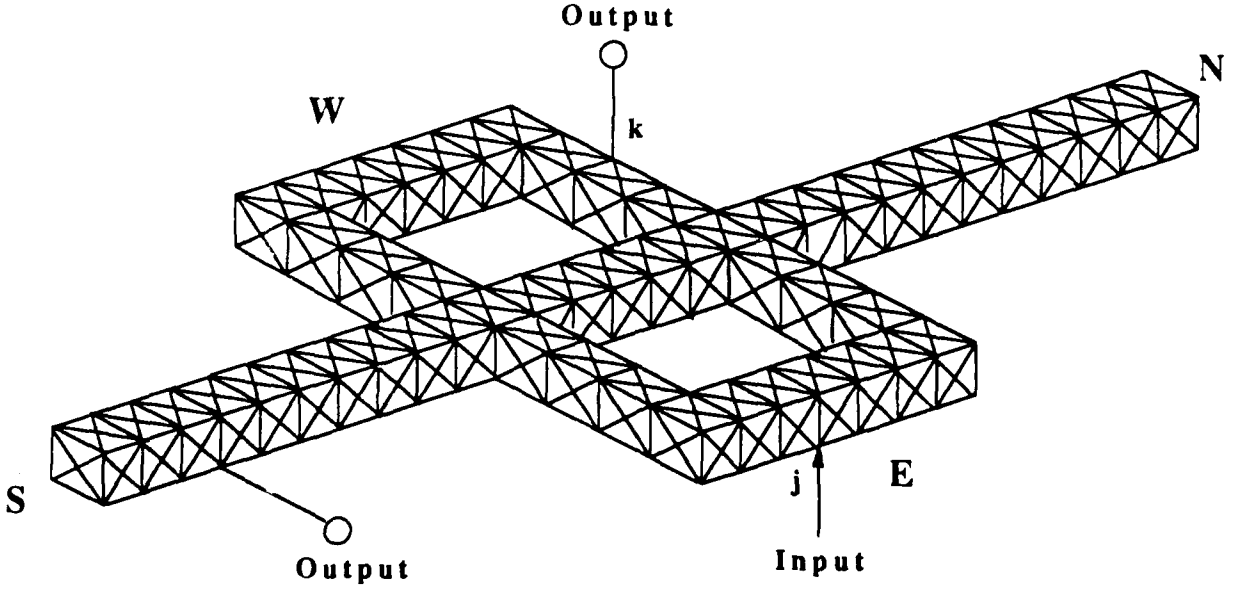

Fig.8 Schematic of an example space structure.

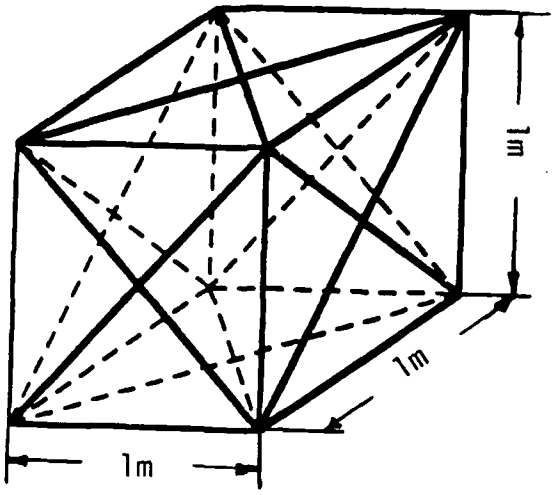

Fig.9 A truss unit.

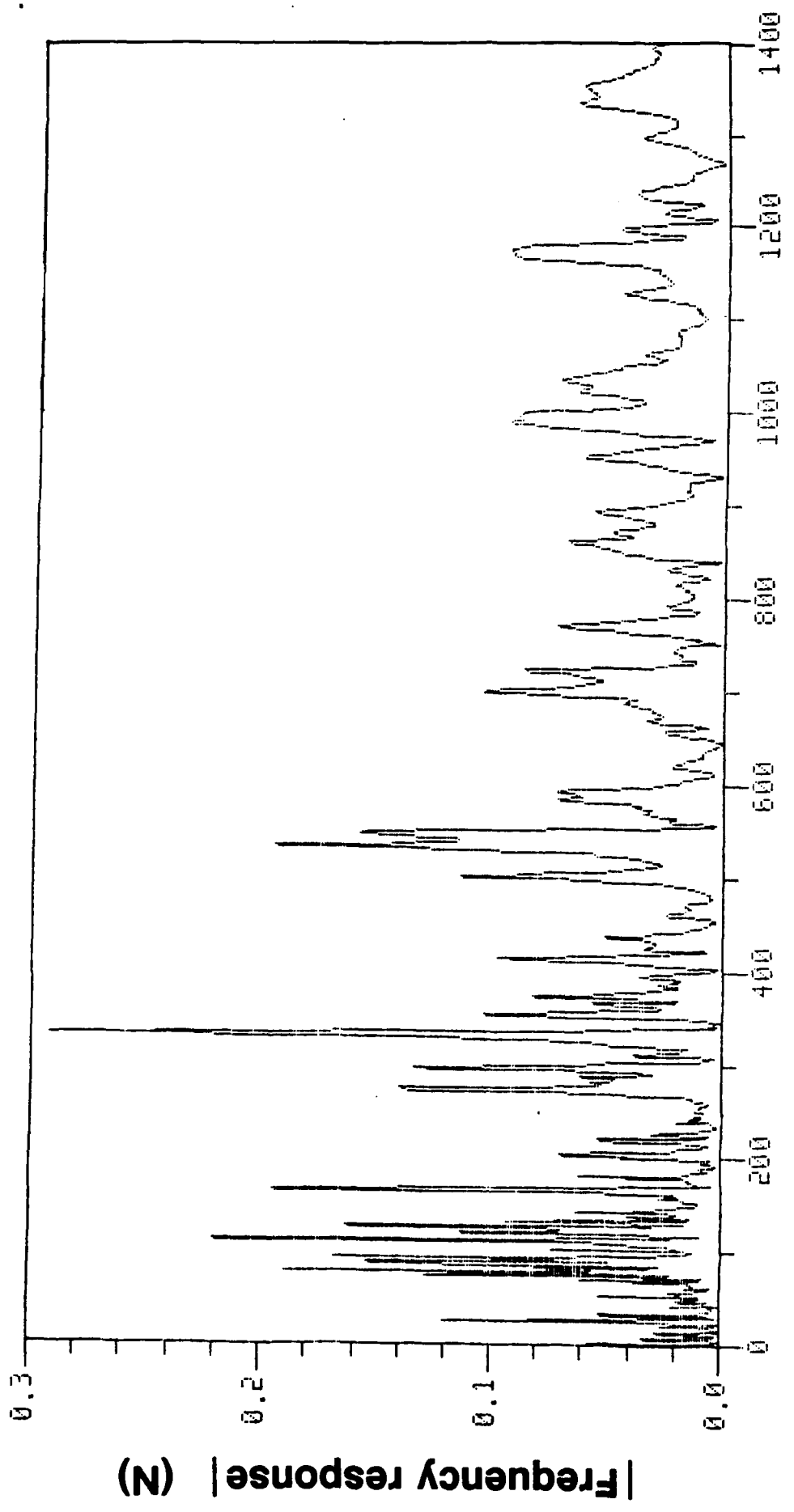

Fig.10 Amplitude of frequency response of a shear force at station k.

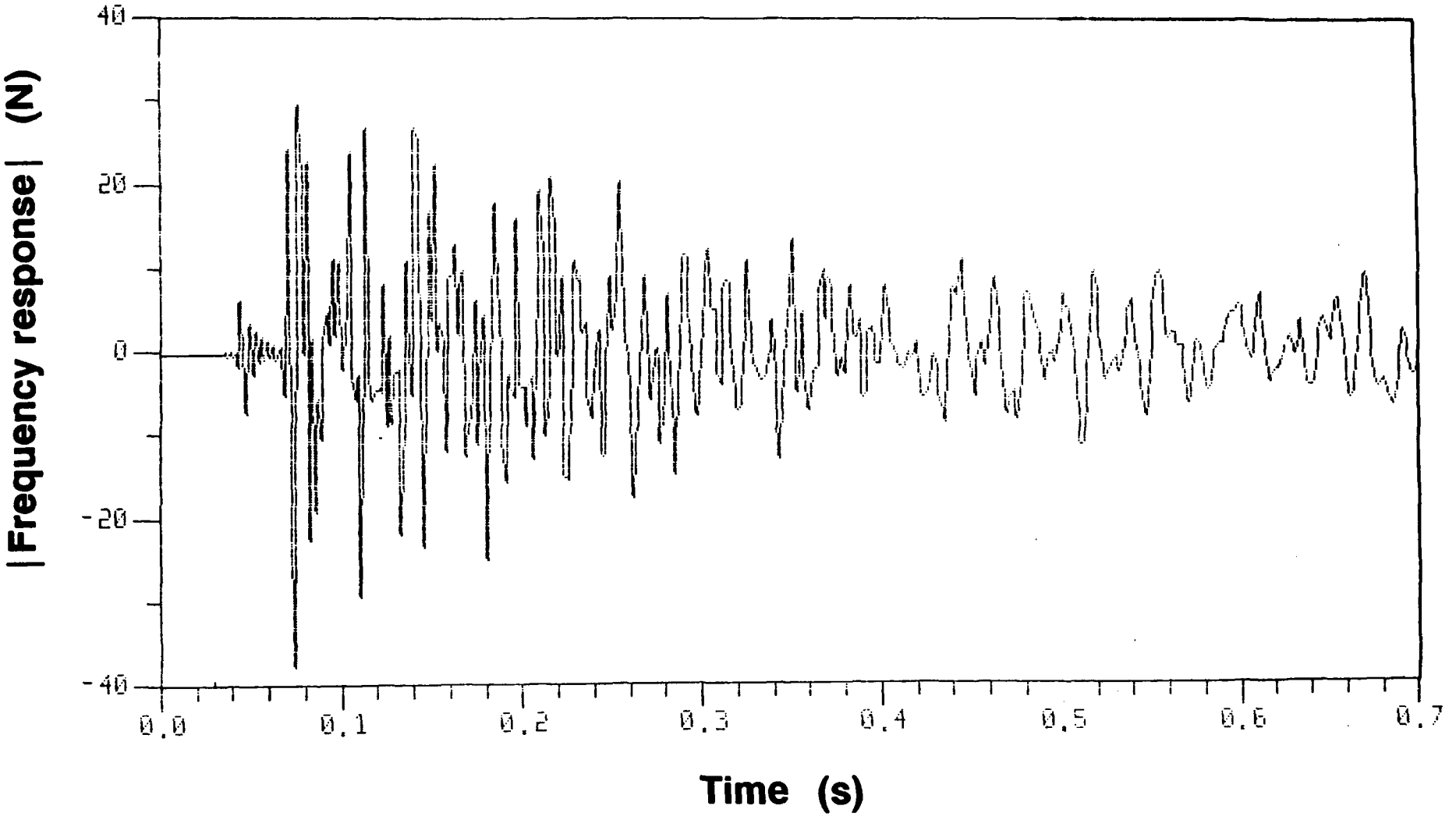

Fig.11 Impulse response of a shear force at station k.

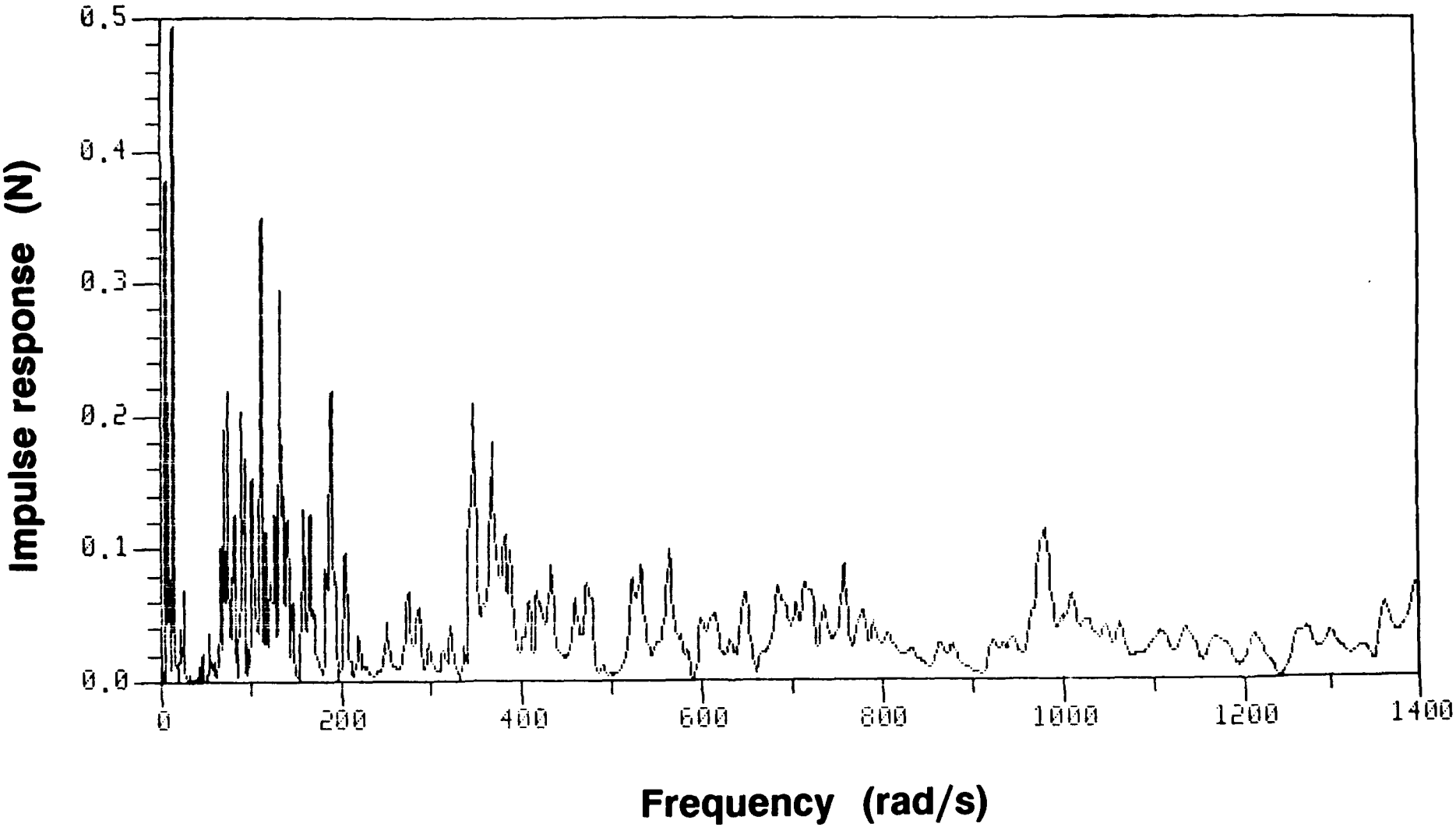

Fig.12 Amplitude of frequency response of a shear force at station h.

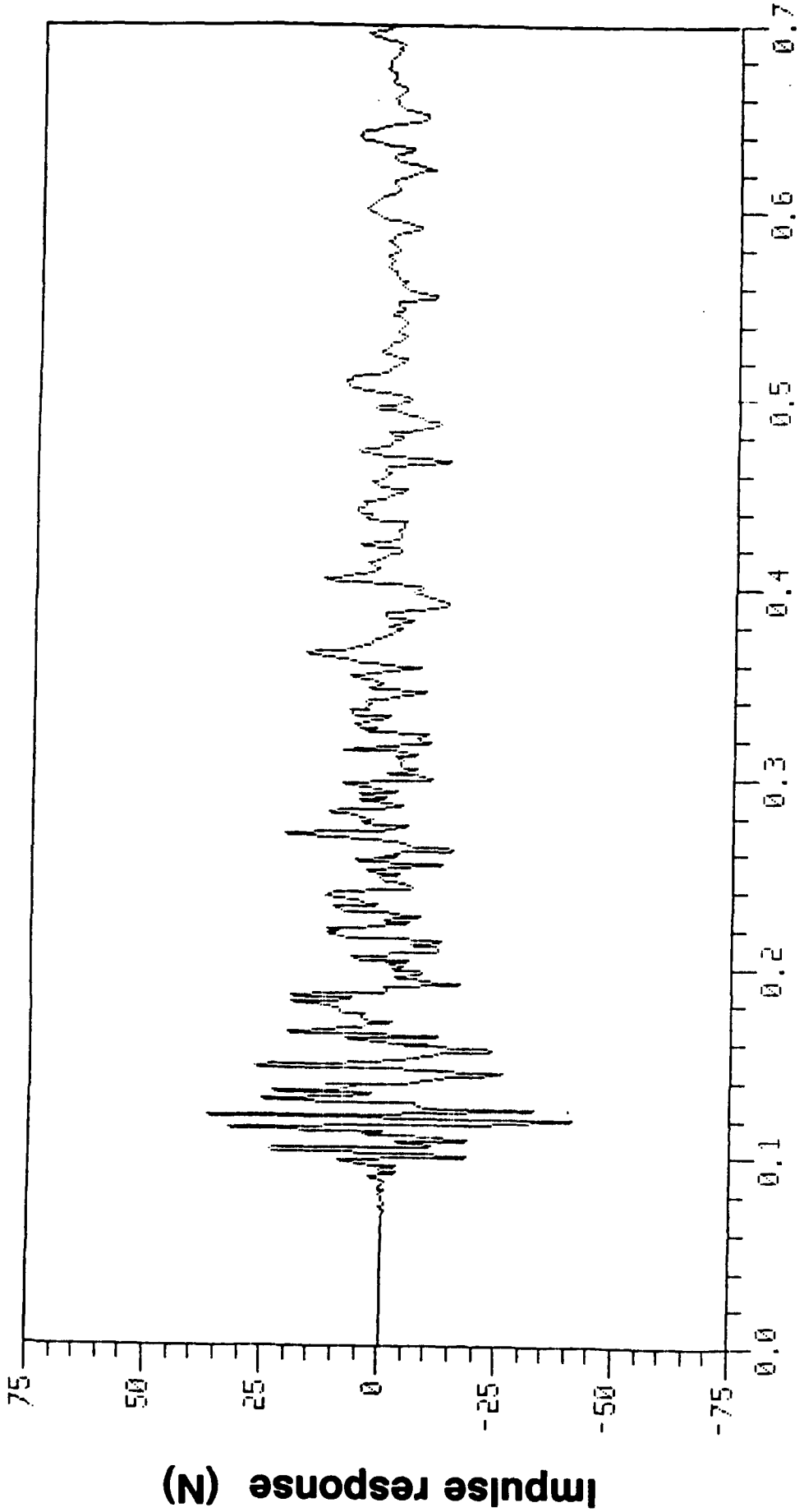

Fig.13 Impulse response of a shear force at station h.

LOCALIZATION OF WAVE PROPAGATION IN DISORDERED PERIODIC STRUCTURES

Due to material, geometric and manufacturing variabilities, a structure designed to be periodic can never be exactly periodic. The departure from ideal periodicity is known as disorder, which must be taken into account in a realistic analysis.

The ability to transmit disturbances indefinitely within the wave-passage bands is reduced when the ideal periodicity in a periodic structure is disrupted. This is known as the localization effect, first predicted by Anderson in a celebrated paper[11] concerning the transport of electrons in an atomic lattice, which is essentially a disordered three-dimensional periodic system. Anderson's work has found important applications in solid state physics. Since then, numerous papers on localization have appeared in the physics literature[12].

Obviously, localization also occurs in disordered periodic structural systems, but its theoretical investigation is more difficult than that of a one-dimensional atomic lattice since governing equations for structural systems are generally more complex. Using the models of a chain of coupled pendula and a vibrating string constrained by attached masses and springs, Hodges[13] provided an excellent explanation for the confinement of vibration and for localized normal modes as a result of structural irregularity. Subsequently, he and Woodhouse[14] calculated the so-called localization factor for one of the systems, characterizing the average exponential decay of vibration amplitude with respect to the distance from the disturbance. Two perturbation schemes were devised to treat the cases of weak and strong localizations, depending on the relative measures of disorder and internal (namely, unit-to-unit) coupling.

Pierre[15] also calculated the localization factor for both weak and strong localization, using both the wave propagation and normal mode formulations and

obtained essentially same results. He devised two perturbation schemes to treat the two cases when the ratio of the disorder measure to the internal coupling measure is either large or small. As expected, his results were not very accurate when this ratio is of order one.

The first analysis of a generic disordered periodic system was given by Kissel[16], making use of the concept of wave transmission and reflection, and a limit theorem on the product of random matrices due to Furstenberg[17]. For a wave motion propagating at a wave-passage frequency, no reflection would occur at the unit-to-unit interface if the system were exactly periodic. When two adjoining units are not identical, total transmission is no longer possible, and some reflection will take place at the interface. However, Kissel's analysis requires that the reflection be small; thus, his results are valid only for the case of weak localization.

Unlike previous investigators, Kissel has also explored the case of multi-coupling; namely, the internal coupling which permits the transmission of several types of waves. An outline was provided of an approach based on the multiplicative ergodic theorem of Oseledets[18]. Unfortunately, the theorem only predicts the existence of a localization factor (analogous to the Lyapunov exponent in the time domain, of interest to Oseledets), without providing the necessary clues as how it can be calculated.

The ability to treat a generic system is clearly very desirable, since the analysis is applicable to a general class of problems, not restricted to a specific type of governing equations. Furthermore, it appears easier to extend such an analysis to the case of multi-coupling which is likely to occur in many practical structural systems. Thus, it is also the objective of the present research to calculate the localization factor for a generic disordered periodic structure. A new perturbation scheme is developed here which permits successive

improvement of the accuracy, making it applicable to either weak, moderate or strong localization. The additional accuracy is obtained by taking into account reflections from additional nearby cells. Account is also taken of structural damping; thus, the results are more useful to practicing engineers. The key to the successful development of a simple theory under rather general settings is the substitution of ensemble averages for sequential averages of certain statistical properties of the structure on the basis of spatial ergodicity. The simplicity of the new method is illustrated by applying it to a multiply supported Euler-Bernoulli beam with an additional torsional spring at each support. The accuracy of the results is substantiated by Monte-Carlo simulations. Only mono-coupling at the unit-to-unit interfaces is considered in detail. The case of multicoupling will be considered in the future.

Wave Transmission and Reflection Matrices

Consider two typical cell-units in a disordered periodic structure, denoted as cells n and n+1 and shown in Fig. 1a. The relation between the state vector at the left end of cell-unit n and that at the left end of cell-unit n+1 may be written as follows

$$\begin{Bmatrix} w(n+1_\ell) \\ f(n+1_\ell) \end{Bmatrix} = [T(n)] \begin{Bmatrix} w(n_\ell) \\ f(n_\ell) \end{Bmatrix} \tag{1}$$

where each w is a p-dimensional vector of generalized displacements, each f is a p-dimensional vector of generalized forces, and [T(n)] is a 2px2p transfer matrix associated with the nth cell. It is implied in Eq.(1) that the motion is time-wise sinusoidal, and the displacements and forces are interpreted as their complex-valued amplitudes. Because of disorder, [T(n)] is generally different from the ideal transfer matrix [T] associated with the ideal design condition of exact periodicity. Nevertheless, it is always possible to write

$$[T(n)] = [P(n)][T] \tag{2}$$

which means that the effect of disorder in the nth cell can be lumped at its right end and represented by a "point" transfer matrix [P(n)]. In other words, the original system shown in Fig. 1a can be replaced by an equivalent system shown in Fig.1b. In typical transfer matrix analysis[19], a point transfer matrix is used to relate state vectors on the two sides of a structural discontinuity which may arise from a concentrated mass, spring, damper, etc. However, [P(n)] in Eq.(2) is merely a mathematical device, and it may even correspond to, e.g., a negative mass.

Refer to Fig. 1b and write

$$\begin{Bmatrix} w(n_r) \\ f(n_r) \end{Bmatrix} = [T] \begin{Bmatrix} w(n_\ell) \\ f(n_\ell) \end{Bmatrix} \tag{3-a}$$

$$\begin{Bmatrix} w(n+1_\ell) \\ f(n+1_\ell) \end{Bmatrix} = [P(n)] \begin{Bmatrix} w(n_r) \\ f(n_r) \end{Bmatrix} \tag{3-b}$$

Each state vector in Eq.(3-a) can be transformed into a wave vector using

$$\begin{Bmatrix} w(n_\ell) \\ f(n_\ell) \end{Bmatrix} = [D] \begin{Bmatrix} \mu^r(n_\ell) \\ \mu^\ell(n_\ell) \end{Bmatrix} \tag{4-a}$$

$$\begin{Bmatrix} w(n_r) \\ f(n_r) \end{Bmatrix} = [D] \begin{Bmatrix} \mu^r(n_r) \\ \mu^\ell(n_r) \end{Bmatrix} \tag{4-b}$$

where the columns in the transformation matrix [D] are the eigenvectors of [T]. These eigenvectors must be arranged in a particular order, which will become apparent in the subsequent development. We then obtain a wave transfer relationship

$$\begin{Bmatrix} \mu^r(n_r) \end{Bmatrix} = [D]^{-1}[T][D] \begin{Bmatrix} \mu^r(n_\ell) \end{Bmatrix} = \begin{bmatrix} \lambda_1 & & 0 \\ & \lambda_2 & \\ & \ddots & \\ 0 & & \end{bmatrix} \begin{Bmatrix} \mu^r(n_\ell) \end{Bmatrix} \tag{5}$$

$$\mu^{\ell}(n_r) \qquad \mu^{\ell}(n_\ell) \qquad \begin{bmatrix} 0 & \cdot \\ & \lambda_{2p} \end{bmatrix} \mu^{\ell}(n_\ell)$$

in which λ_j, j=1, ..., 2p are the eigenvalues of the ideal transfer matrix [T]. Each λ_j represents the ratio of complex-valued amplitudes of one type of wave at the two ends of an ideal cell-unit. Since damping generally exists in a physical structure, the magnitude of a wave decreases when propagating across a cell. Thus, each eigenvalue accounts for the reduction of the wave magnitude, as well as the change of phase from one side of an ideal cell-unit to another. It is known that eigenvalues of a transfer matrix are reciprocal pairs[3]. For every λ_j, there exists another $\lambda_k = \lambda_j^{-1}$. If $|\lambda_j| < 1$, then $|\lambda_k| = |\lambda_j|^{-1} > 1$. They correspond to two identical types of waves, except that one is right-going and the other is left-going. The limiting case $|\lambda_j| = 1$ can only occur in an undamped structure, and only at a frequency in one of the wave-passage frequency bands.

We arrange the order of eigenvectors in [D] such that the corresponding eigenvalues are in an ascending order; thus $|\lambda_j| < 1$, if j = 1, 2, ..., p and $|\lambda_j| > 1$, if j = p+1, p+2, ..., 2p. Eq. (5) may then be re-written as follows

$$\begin{Bmatrix} \mu^{r}(n_r) \\ \mu^{\ell}(n_r) \end{Bmatrix} = \begin{bmatrix} \Lambda & 0 \\ 0 & \Lambda^{-1} \end{bmatrix} \begin{Bmatrix} \mu^{r}(n_\ell) \\ \mu^{\ell}(n_\ell) \end{Bmatrix} \tag{6}$$

where

$$\Lambda = \begin{bmatrix} \lambda_1 & & 0 \\ & \cdot & \\ & & \cdot \\ 0 & & \lambda_p \end{bmatrix} \tag{7}$$

Or, alternatively,

$$\begin{Bmatrix} \mu^{\ell}(n_\ell) \\ \mu^{r}(n_r) \end{Bmatrix} = [S] \begin{Bmatrix} \mu^{r}(n_\ell) \\ \mu^{\ell}(n_r) \end{Bmatrix} \tag{8}$$

with

$$[S] = \begin{bmatrix} 0 & \Lambda \\ \Lambda & 0 \end{bmatrix} \tag{9}$$

The meanings of the superscripts r and ℓ associated with the wave vectors μ are now clear; they indicate the right-going and the left-going wave groups, respectively, transmitted from one end of an ideal cell to the other, as shown schematically in Fig. 2. In fact, Eq.(8) has been written to suggest that $\mu^r(n_\ell)$ and $\mu^\ell(n_r)$ are the input waves and $\mu^\ell(n_\ell)$ and $\mu^r(n_r)$ are output waves, as viewed by the structural unit which is characterized by [S].

Similar transformation of the state vectors in Eq.(3-b) to wave vectors results in

$$\begin{Bmatrix} \mu^r(n+1_\ell) \\ \mu^\ell(n+1_\ell) \end{Bmatrix} = [Q(n)] \begin{Bmatrix} \mu^r(n_r) \\ \mu^\ell(n_r) \end{Bmatrix} \tag{10}$$

where

$$[Q(n)] = [D]^{-1}[P(n)][D] = [D]^{-1}[T(n)][D] \begin{bmatrix} \Lambda^{-1} & \\ & \Lambda \end{bmatrix} \tag{11}$$

Eq.(10) can be re-cast in the form of Eq.(8); namely,

$$\begin{Bmatrix} \mu^\ell(n_r) \\ \mu^r(n+1_\ell) \end{Bmatrix} = [S(n)] \begin{Bmatrix} \mu^r(n_r) \\ \mu^\ell(n+1_\ell) \end{Bmatrix} \tag{12}$$

The elements in [S(n)] can be obtained from those of [Q(n)] as follows

$$s_{11} = - q_{22}^{-1} q_{21} \tag{13a}$$

$$s_{12} = q_{22}^{-1} \tag{13b}$$

$$s_{21} = q_{11} - q_{12} q_{22}^{-1} q_{21} \tag{13c}$$

$$s_{22} = q_{12} q_{22}^{-1} \tag{13d}$$

In Eqs. (13a-13d) s_{ij} and q_{ij} are pxp submatrices of [S(n)] and [Q(n)], respectively, and the argument (n) is omitted in denoting the submatrices for simplicity.

It is physically meaningful to re-name the submatrices of [S(n)] as $r^r(n)=s_{11}$, $t^\ell(n)=s_{12}$, $t^r(n)=s_{21}$, and $r^\ell(n)=s_{22}$, and re-write Eq.(12) as

$$\begin{Bmatrix} \mu^\ell(n_r) \\ \mu^r(n+1_\ell) \end{Bmatrix} = \begin{bmatrix} r^r(n) & t^\ell(n) \\ t^r(n) & r^\ell(n) \end{bmatrix} \begin{Bmatrix} \mu^r(n_r) \\ \mu^\ell(n+1_\ell) \end{Bmatrix} \tag{14}$$

The submatrices t and r are called the transmission and reflection matrices, respectively. The superscript for each of these submatrices signifies the direction of an incoming wave group to be transmitted or reflected. For example, $t^r(n)$ is a transmission matrix for an incoming wave group traveling in the right direction.

Matrix [S(n)], which contains the transmission and reflection submatrices, is known as a scattering matrix. This particular scattering matrix characterizes the effects of disorder in cell n which are lumped at the right end of cell n, as shown schematically in Fig.2. In wave mechanics, the concept of a scattering matrix is quite general; it characterizes the behavior of any identifiable structural element. In fact, matrix [S] in Eq.(8) is also a scattering matrix, in which the transmission and reflection matrices are $t^r=t^\ell=\Lambda$ and $r^r=r^\ell=0$. These submatrices of [S] are also related to those of a matrix [Q] according to Eqs.(13a-d), although in this special case

$$[Q] = \begin{bmatrix} \Lambda & 0 \\ 0 & \Lambda^{-1} \end{bmatrix} \tag{15}$$

It is interesting to remark that all scattering matrices are symmetric, a consequence of the reciprocity theorem for linear acoustic systems.

For a chain of cell units, 1 through N, we may write

$$\begin{Bmatrix} \mu^r(N+1_\ell) \\ \mu^\ell(N+1_\ell) \end{Bmatrix} = [Q(N,1)] \begin{Bmatrix} \mu^r(1_\ell) \\ \mu^\ell(1_\ell) \end{Bmatrix} \tag{16}$$

where

$$[Q(N,1)]=[Q(N)][Q][Q(N-1)][Q]...[Q(1)][Q] \tag{17}$$

and where [Q(n)] and [Q] are given in Eqs. (11) and (15), respectively. Eq.(16) can be re-cast in the form of

$$\begin{Bmatrix} \mu^\ell(1_\ell) \\ \mu^r(N+1_\ell) \end{Bmatrix} = [S(N,1)] \begin{Bmatrix} \mu^r(1_\ell) \\ \mu^\ell(N+1_\ell) \end{Bmatrix} \tag{18}$$

in which

$$[S(N,1)] = \begin{bmatrix} r^r(N,1) & t^\ell(N,1) \\ t^r(N,1) & r^\ell(N,1) \end{bmatrix} \tag{19}$$

Elements of matrix [S(N,1)] are related to those of matrix [Q(N,1)] according to Eqs. (13a-d). From the second row of Eq.(18), we obtain

$$\mu^r(N+1_\ell) = t^r(N,1)\mu^r(1_\ell) + r^\ell(N,1)\mu^\ell(N+1_\ell) \tag{20}$$

The Case of Mono-Coupling

We shall now consider the case of mono-coupling in more detail. In this case the wave transfer matrices Q and the scattering matrices S become 2x2, and the transmission and reflection matrices reduce to the transmission and reflection coefficients. Moreover, we shall assume for the time being that cells N+1, N+2, ..., ∞ are without disorder; thus $\mu^\ell(N+1_\ell)=0$. Then Eq.(20) is simplified to

$$\mu^r(N+1_\ell) = t^r(N,1)\mu^r(1_\ell) \tag{21}$$

The localization factor is defined as

$$\gamma = - \lim_{\substack{N\to\infty \\ \mu^{\ell}(N+1_{\ell}) = 0}} \frac{1}{N} \ell n \left| \frac{\mu^{r}(N+1_{\ell})}{\mu^{r}(1_{\ell})} \right| \tag{22}$$

Upon using Eq.(21)

$$\gamma = - \lim_{N\to\infty} \frac{1}{N} \ell n \left| t^{r}(N,1) \right| \tag{23}$$

It implies that, if the above limit exists, the transmitted wave has an average exponential decaying rate of γ per cell-unit. This simple result can also be derived from an application of Furstenberg's theorem on products of random matrices[17].

In passing, we remark that, for the mono-coupling case, $t^{r}(N,1) = t^{\ell}(N,1)$ as can be proved from Eqs.(13a-d) and from the fact that $|Q(N,1)| = 1$ since $[Q(N,1)]$ is a transfer matrix[3].

Several specific cases will now be considered in the order of increasing complexity:

(1) Small reflections --- If all the reflection coefficients due to disorder are small, such that the effect of multiple reflections is negligible, then $t^{r}(N,1)$ can be approximated by

$$t^{r}(N,1) = t^{r}(1)\ t^{r}(2) \ \ldots\ t^{r}(N)\lambda^{N} \tag{24}$$

From Eq. (13b), $t^{r}(n)=t^{\ell}(n)=t(n)=q_{22}^{-1}(n)$. Whence

$$\gamma = - \ell n |\lambda| + \lim_{N\to\infty} \frac{1}{N} \sum_{n=1}^{N} \ell n \left| q_{22}(n) \right| \tag{25}$$

For disordered cells, each uncertain parameter may be represented as a mean (or nominal value) plus a random variable. Then $q_{22}(n)$ are functions of such random variables which may be denoted by

$$q_{22}(n) = q_{22}[X(n)] \tag{26}$$

where $X(n) = \{X_1(n), X_2(n), \ldots, X_k(n)\}$ is a vector of random variables with zero means. It is reasonable to assume that $X_j(n)$ for different n are independent and identically distributed, and that they form an ergodic sequence. Then the sequential averages in Eq.(25) may be replaced by ensemble averages; namely,

$$\gamma = - \ell n \mid \lambda \mid + \int \ell n \mid q_{22}(x) \mid p(x)\, dx \tag{27}$$

where $p(x)$ is the probability density of $X(n)$ and the integrations are carried out in the domain of the random vector $X(n)$. Eqs.(25) and (27) are equivalent with probability one. If $X(n)$ is a k-vector, the integral in Eq.(27) is actually a k-fold integral. Given the forms of $q_{22}[X(n)]$ and the probability distribution of $X(n)$, the integral can be evaluated at least numerically. In simple cases, it can often be carried out in closed form, as shown later in an example.

If the system disorder is also small, then Eq.(27) may be approximated by

$$\gamma = - \ell n \mid \lambda \mid + \frac{\sigma_i^2}{2} \left\{ \frac{\partial^2}{\partial x_i^2} \ell n \mid q_{22}(x) \mid \right\}_{x = 0} \tag{28}$$

where σ_i^2 are the variances of $X_i(n)$. If, in addition, the structure is undamped and γ is evaluated at a wave-passage frequency, then $\mid \lambda \mid = 1$, and Eq. (28) reduces to

$$\gamma = \frac{\sigma_i^2}{2} \left\{ \frac{\partial^2}{\partial X_i^2} \ell n \mid q_{22}(x) \mid \right\}_{X=0} \tag{29}$$

Eq.(29) has been obtained previously by Kissel[16].

It should be emphasized that Eq.(27) is valid only for small reflection coefficients which imply that localization is weak. Eq.(28) requires both small reflection coefficients and small disorder, and Eq.(29) requires additionally a

zero damping and a wave-passage frequency.

(2) Moderate reflections -- If the reflection coefficients due to disorder are not sufficiently small, the approximation Eq.(24) may not be adequate. For improved accuracy, certain multiple reflections will be considered. As shown in Fig. 3, the right-going wave $\mu^r(n_r)$ gives rise to a right-going transmitted wave $t(n)\mu^r(n_r)$ and a left-going reflected wave $r(n)\mu^r(n_r)$. The reflected wave travels through cell n and is itself partially reflected back at the interface between cells n and n-1. This back-reflected wave travels also through cell n, whereupon it splits again into reflected and the transmitted parts. The latter is clearly $t(n)\lambda^2 r^{\ell}(n-1)r^r(n)\mu^r(n_r)$, and the former travels back through cell n, etc. Summing up all the right-going waves which pass through the interface between cells n and n+1, we obtain

$$\mu^r(n+1_{\ell}) = t(n)\{1+\lambda^2\, r^{\ell}(n-1)r^r(n)+[\lambda^2\, r^{\ell}(n-1)r^r(n)]^2+\ldots\}\mu^r(n_r)$$

$$= \frac{t(n)}{1 - \lambda^2\, r^{\ell}(n-1)\, r^r(n)}\mu^r(n_r) \tag{30}$$

Thus

$$t^r(N,1) = \prod_{n=1}^{N} \frac{t(n)\lambda}{1 - \lambda^2\, r^{\ell}(n-1)\, r^r(n)} \tag{31}$$

It follows from Eqs.(23) and (13a-d), and the ergodicity assumption,

$$\gamma = -\ell n\,|\,\lambda\,| + \int \ell n\,|\,q_{22}(x)\,|\,p(x)dx$$

$$+ \iint \ell n\,\Big|\,1 + \frac{\lambda^2\, q_{12}(x_2)q_{21}(x_1)}{q_{22}(x_2)\, q_{22}(x_1)}\,\Big|\,p(x_1)p(x_2)\, dx_1dx_2 \tag{32}$$

The third term is seen to provide added accuracy over Eq.(27). Eq.(32) is valid for the case of moderate localization.

(3) Strong reflection -- Eq.(32) may still be inadequate if the reflection coefficients are relatively large (although each cannot have a magnitude greater than one). Higher accuracies, however, can always be obtained by including more reflection terms in the formulation. It can be shown that if the effect of reflection at the interface between cells n-1 and n-2 is also taken into consideration, then

$$\mu^r(n+1_\ell) = t(n)\left[\frac{1}{1-a} + \frac{c}{(1-a)(1-b)(1-c)}\right]\mu^r(n_r) \tag{33}$$

where

$$a = \lambda^2\, r^\ell(n-1)r^r(n) \tag{34a}$$

$$b = \lambda^2\, r^\ell(n-2)r^r(n-1) \tag{34b}$$

$$c = t^2(n-1)\lambda^4\, r^\ell(n-2)r^r(n) \tag{34c}$$

Again, using Eqs.(13a-d) and invoking the ergodicity assumption,

$$\gamma = -\ell n\,|\lambda| + \int \ell n\,|q_{22}(x)|\,p(x)\,dx$$

$$-\iiint \ell n\left|\frac{1}{1+f_1(x_1,x_2)} - \frac{f_2(x_1,x_2,x_3)}{[1+f_1(x_1,x_2)][1+f_1(x_2,x_3)][1+f_2(x_1,x_2,x_3)]}\right|$$

$$p(x_1)p(x_2)p(x_3)\,dx_1dx_2dx_3 \tag{35}$$

where

$$f_1(x_1,x_2) = \frac{\lambda^2\, q_{12}(x_2)q_{21}(x_1)}{q_{22}(x_1)q_{22}(x_2)} \tag{36a}$$

$$f_2(x_1,x_2,x_3) = \frac{\lambda^4\, q_{12}(x_3)q_{21}(x_1)}{q_{22}^2(x_2)q_{22}(x_3)q_{22}(x_1)} \tag{36b}$$

Formulas of still higher accuracies can be derived in an analogous manner.

An Example

For illustration, the above theory is applied to an Euler-Bernoulli beam on evenly spaced hinge supports and with an additional torsional spring at each support, as shown in Fig. 4. In order to focus our attention on certain key issues in the theory without being obscured by unnecessary complexities, it is assumed that the beam is undamped and that only the torsional spring stiffnesses are random and are described by

$$k_n = k_o[1+ X(n)] \qquad n = 1, 2, \ldots \tag{37}$$

where k_o is the average k_n and $X(n)$ are random variables with zero means. The other physical parameters are assumed to be deterministic, including the distances between neighboring supports ℓ, the bending rigidity of the beam EI, and the mass of the beam per unit length m. The theory is, of course, applicable when several or all the parameters are random.

Several choices can be made for a typical cell-unit in the analysis. The one selected for the following discussion is a typical beam element between two neighboring supports plus the entire right spring. The entire left spring is treated as belonging to the preceeding cell. Then the transfer matrix for the nth cell is given by[3].

$$[T(n)] = \begin{bmatrix} \beta & \frac{\alpha}{\nu} \\ -\frac{\nu(1-\beta^2)}{\alpha} + \frac{\beta}{\delta}[1+X(n)] & \beta + \frac{\alpha}{\delta\nu}[1 + X(n)] \end{bmatrix} \tag{38}$$

where $\delta = \frac{EI}{\ell k_o}$, $\nu = \ell(\frac{\omega^2 m}{EI})^{1/4}$, ω = frequency

$$\alpha = \frac{\cosh\nu \cos\nu - 1}{\sinh\nu - \sin\nu} \tag{39a}$$

and

$$\beta = \frac{\sinh\nu \cos\nu - \cosh\nu \sin\nu}{\sinh \nu - \sin \nu} \tag{39b}$$

The non-dimensional δ is called the internal (cell-to-cell) coupling parameter, which is a measure of relative resistance against a rotation at a support between the beam element and an average torsional spring. If k_o is very large such that δ is very small, then there is little cell-to-cell coupling, and strong localization is expected to occur[15].

The transfer matrix [T] for the ideal cell-unit without disorder and the point transfer matrix [P(n)] lumping the effect of disorder are obtained as follows

$$[T] = \begin{bmatrix} \beta & \frac{\alpha}{\nu} \\ -\frac{\nu(1-\beta^2)}{\alpha} + \frac{\beta}{\delta} & \beta + \frac{\alpha}{\delta\nu} \end{bmatrix} \tag{40-a}$$

$$[P(n)] = \begin{bmatrix} 1 & 0 \\ \frac{X(n)}{\delta} & 1 \end{bmatrix} \tag{40-b}$$

The eigenvalues of transfer matrix [T] are a reciprocal pair which may be denoted conveniently by $e^{\pm i\theta}$. It can be shown that θ can be found from[3]

$$\cos\theta = \beta + \frac{\alpha}{2\delta\nu} \tag{41}$$

and the wave-passage frequency bands are determined by the inequality

$$-1 \leq \beta + \frac{\alpha}{2\delta\nu} \leq 1 \tag{42}$$

The wave transfer matrix [Q(n)] is obtained from

$$[Q(n)] = \begin{bmatrix} 1-iAX(n) & -iAX(n) \\ iAX(n) & 1+iAX(n) \end{bmatrix} \tag{43}$$

where $A = \alpha/(2\delta\nu\sin\theta)$.

The following physical properties have been used in the numerical calculations: $\ell = 0.1651$m, $m = 1.8043$ kg/m, and $EI = 0.3143$ N-m^2. In addition, X(n) are assumed to be identically and uniformly distributed between $-\sqrt{3}\sigma$ and $\sqrt{3}\sigma$ where σ is the standard deviation of X(n).

Substituting Eq.(43) into Eq.(27), we obtain an approximate localization factor for the case of wave-passage frequency and weak localization.

$$\gamma = \frac{1}{2}\ell n(1+3A^2\sigma^2)-1 + \frac{1}{\sqrt{3}A\sigma}\tan^{-1}(\sqrt{3}A\sigma) \tag{44}$$

where σ^2 is the variance of X(n) which is assumed to be the same for all n. If, in addition, the disorder is small, we obtain from Eq.(29).

$$\gamma = \frac{\alpha^2\sigma^2}{8\delta^2\nu\sin^2\theta} \tag{45}$$

For other cases for which the use of Eq.(27), Eq. (32) or Eq.(35) is more appropriate, numerical integrations are generally required using an assumed probability density for X(n).

The computed localization factors in the first four wave-passage frequency bands are shown in Fig.5(a) and (b) for δ=1, σ=0.1 and for δ=0.1, σ=0.1, respectively. Except for frequencies very close to the lower boundary of a wave-passage frequency band (not shown in Fig.5), all the four equations (27), (29), (32) and (35) yield essentially the same results, and in excellent agreement with those obtained from Monte Carlo simulations, also shown in the figure. That the values of the localization factors are below 0.02 is an

indication of weak localization in these cases. At the lower boundary of a wave-passage frequency band, the deformations of two neighboring spans tend to be out of phase (exactly out of phase for an ideal periodic structure) and the torsional spring at the supports influence the beam motion to a great extent. Therefore even a small disorder of the torsional springs may give rise to strong localization. On the other hand, the deformations of two neighboring spans are nearly in phase at the upper boundary of a wave-passage frequency and the torsional springs have little effect on the beam motion. Hence, their disorder is relatively unimportant.

The Monte-Carlo simulations referred to above were carried out by multiplying a large number of random wave transfer matrices at a given frequency to obtain one realization of the wave transfer matrix for the overall N-span system according to Eq.(17) and thus one realization of $t^r(N,1)$. The values of $N^{-1}\ell n \mid t^r(N,1) \mid$ for different realizations were averaged over a sufficient number of realizations to obtain an estimate for the localization factor. This procedure is different from the one adopted by Kissel[16] in which an average is taken of a large number of $\ell n \mid t(n) \mid$ where each $t(n)$ is the transmission coefficient of one realization of a single cell. It is felt that our simulation procedure is physically more meaningful. In our simulations, 300 cells were used in each realization, and the average was taken over 2000 realizations.

Fig.6(a) and (b) depict the computed localization factors for systems with δ=0.01, σ=0.25 and δ=0.01, σ=0.50, respectively, and with frequencies falling within the lower part of the first wave-passage frequency band. It is seen that the closer a frequency is to the lower boundary of the wave-passage frequency band, the more Eqs. (27) and (29) overestimate the localization factor, because the reflection coefficients become larger and the effect of multiple reflection is no longer negligible. By taking the reflections in only one cell on the

immediate left into account, Eq.(32) yields much more accurate results than those of Eqs.(27) and (29) when compared with simulation results. Fig. 6 shows that for a beam system with fixed δ and σ, localization is strong at a frequency very near to the lower boundary of a wave-passage frequency band, and it becomes weaker as the frequency increases. This implies that the disorder to internal coupling ratio (σ/δ) is not the only factor in determining the intensity of localization, as once suggested; the frequency location relative to a wave-passage band is at least another factor. Other factors might be also important in more complicated systems.

Results obtained from Eq.(27) are generally more accurate than those obtained from Eq.(29). However, exceptions can occur, as shown in the higher frequency region in Figs.6(a) and 6(b). This is due to the fact that both equations are approximate. Although Eq.(27) essentially retains more terms in the approximatation, it does not follow that those additional terms will increase the accuracy consistently.

As pointed out above, localization may be strong at frequencies near the lower boundaries of wave-passage frequency bands, even when the disorder is relatively small. Three such cases: (a) δ=0.1, ω=232.5 rad/s, (b) δ=0.01, ω=318.7 rad/s and (c) δ=0.001, ω=339.72 rad/s have been examined in more detail. The results obtained are shown in Fig. 7(a)-(c), respectively, with varying standard deviation of disorder σ. In all these cases Eq.(32) is clearly inadequate. Eq.(35) leads to satisfactory results for cases (b) and (c). For case (a) in which the disorder is also greater, Eq.(35) is still inadequate although it is much superior to Eq.(32). The use of even higher order approximations is suggested.

Concluding Remarks

The successive improvement in accuracy and the inclusion of structural

damping are two important features in the proposed perturbation scheme for the computation of localization factors for disordered periodic structures. The first feature permits a unified approach to any disorder to internal coupling ratio, and at any frequency location relative to the lower boundaries of the wave-passage frequency band. They are shown to be the governing factors for the degree of localization in the illustrative examples. The second feature permits the consideration of practical structures. The formulation based on a generic disordered periodic structure is also an advantage, since it is not restricted to a specific type of system, and it facilitates future extension to the case of multiple coupling between neighboring cells.

References

[1]Miles, J.W., "Vibration of Beams on Many Supports," Journal, Engineering Mechanics Division, ASCE, Vol. 82, EM1, Jan. 1956, pp.1-9.

[2]Lin, Y. K., "Free Vibration of Continuous Beams on Elastic Supports," Journal of Mechanical Science, Vol. 4, September-October, 1962, pp.409-423.

[3]Lin, Y. K. and McDaniel, T. J., "Dynamics of Beam-Type Periodic Structures," Journal of Engineering for Industry, Vol. 91, November, 1969, pp.1133-1141.

[4]Mead, D. J., "Free Wave Propagation in Periodically-Supported Infinite Beam," Journal of Sound and Vibration, Vol. 11, 1970, pp.181-197.

[5]Mead, D. J., "Wave Propagation and Natural Modes in Periodic Systems: I. Mono-Coupled Systems, II. Multi-Coupled Systems, With and Without Damping," Journal of Sound and Vibration, Vol. 40, 1975, pp.1-39.

[6]Yong, Y., and Lin, Y.K., "Propagation of Decaying Waves in Periodic and Piecewise Periodic Structures of Finite Length," Journal of Sound and Vibration, Vol. 129, 1989, pp. 99-118.

[7]Soong, T. T. and Bogdanoff, J. L, "On the Natural Frequencies of a

Disordered Linear Chain of N Degrees of Freedom," Journal of Mechanical Sciences, Vol. 5, 1963, pp.237-265.

[8]Soong, T. T. and Bogdanoff, J. L., "On the Impulsive Admittance and Frequency Response of a Disordered Linear Chain of N-Degrees of Freedom," Journal of Mechanics Sciences, Vol. 6, 1964, pp.225-237.

[9]Lin, Y. K. and Yang, J. N., "Free Vibration of a Disordered Periodic Beam," Journal of Applied Mechanics, Vol. 41, 1974, pp. 383-391.

[10]Yang, J. N., and Lin, Y. K., "Frequency Response Functions of a Disordered Periodic Beam," Journal of Sound and Vibration, Vol. 38, No. 3, 1975, pp. 317-340.

[11]Anderson, P.W., "Absence of Diffusion in Certain Random Lattices," Physical Review, Vol. 109, 1958, pp. 1492-1505.

[12]Lee, P., "Disordered Solids, "Physics Today, Vol. 41, 1988, pp. 22-23.

[13]Hodges, C. H., "Confinement of Vibration by Structural Irregularity," Journal of Sound and Vibration, Vol. 82, No. 3, 1982, pp. 441-444.

[14]Hodges, C. H. and Woodhouse, J., "Vibration Isolation from Irregularity in a Nearly Periodic Structure: Theory and Measurements," Journal of Acoustic Society of America, Vol. 74, No. 3, 1983, pp. 894-905.

[15]Pierre, C., "Weak and Strong Vibration Localization in Disordered Structures: A Statistical Investigation," Proceedings of the 29th SDM AIAA/ASME/AHS/ASCE Conference, April, 1988.

[16]Kissel, G. J., "Localization in Disordered Periodic Structures," Ph.D. Dissertation, Massachusetts Institute of Technology, 1988.

[17]Furstenberg, H., "Noncommuting Random Products," Transactions of the American Mathematical Society, Vol. 108, No. 3, 1963, pp. 377-428.

[18]Oseledets, V. I., "A Multiplicative Ergodic Theorem," Transactions of the Moscow Mathematical Society, Vol. 19, 1968.

[19]Pestel, E. C., and Leckie, F. A., "Matrix Methods in Elastomechanics," McGraw-Hill, New York, 1963.

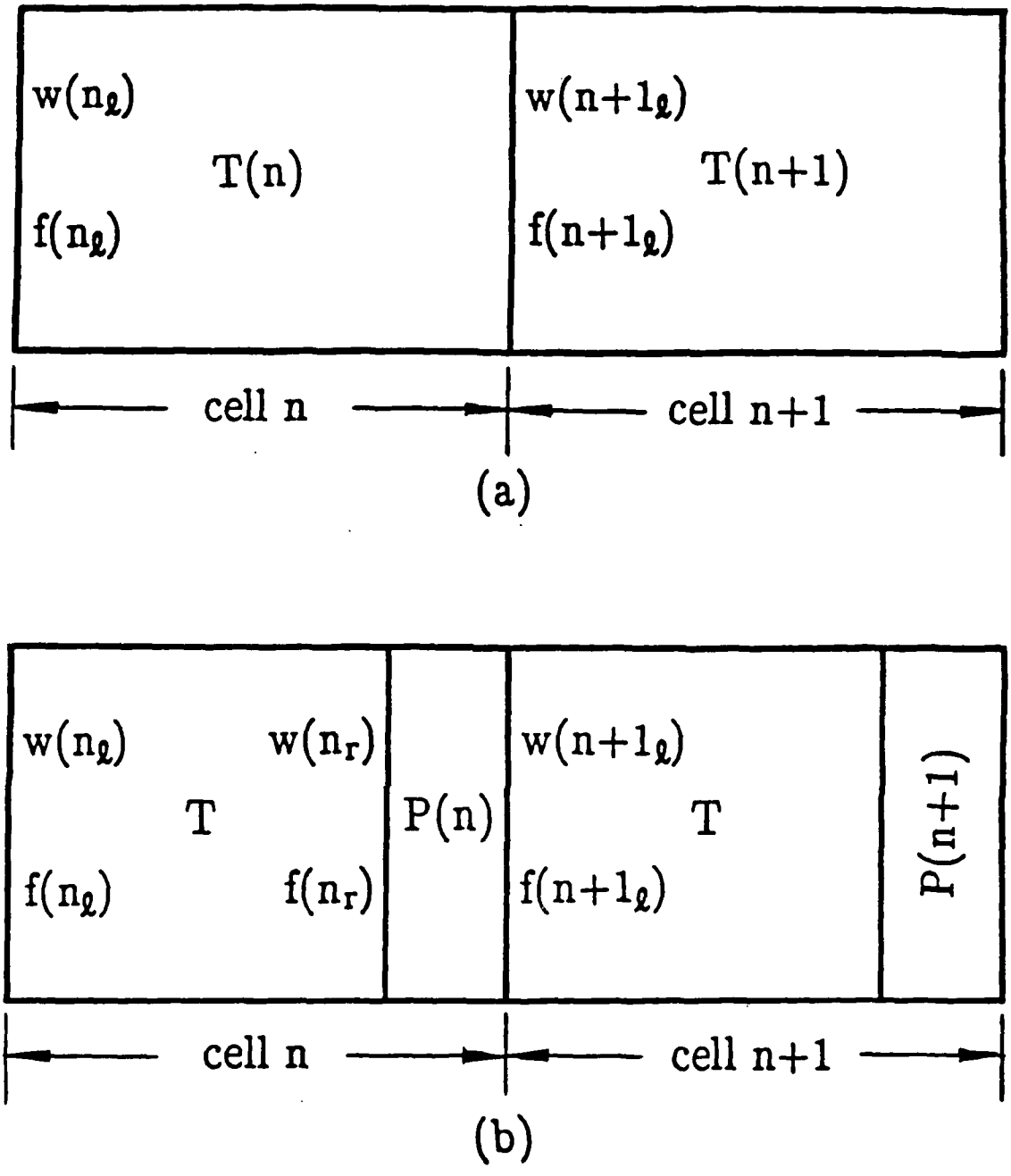

Fig. 1 State vector representation; (a) Original system, (b) Equivalent system.

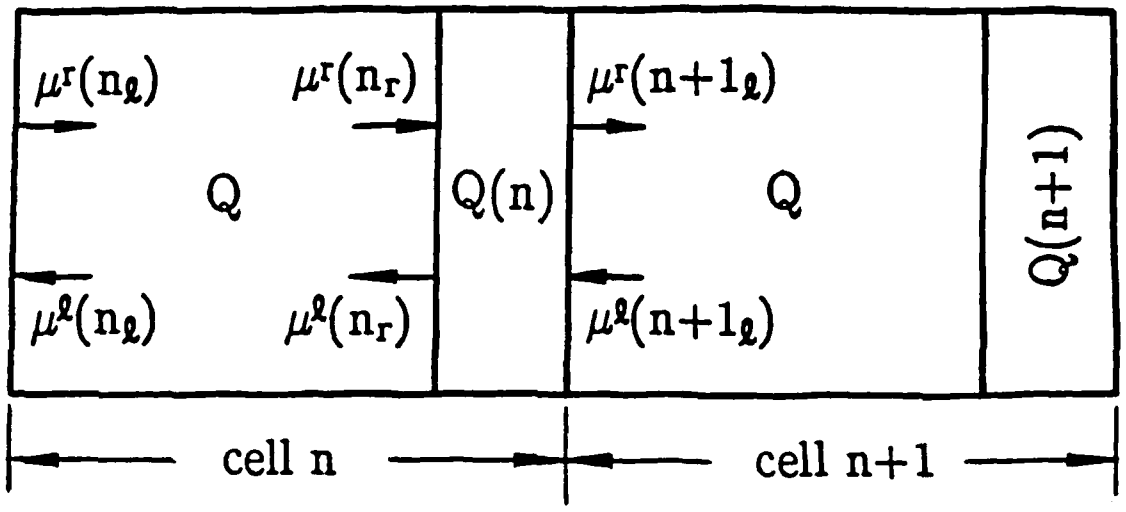

Fig. 2 Wave vector representation, equivalent system.

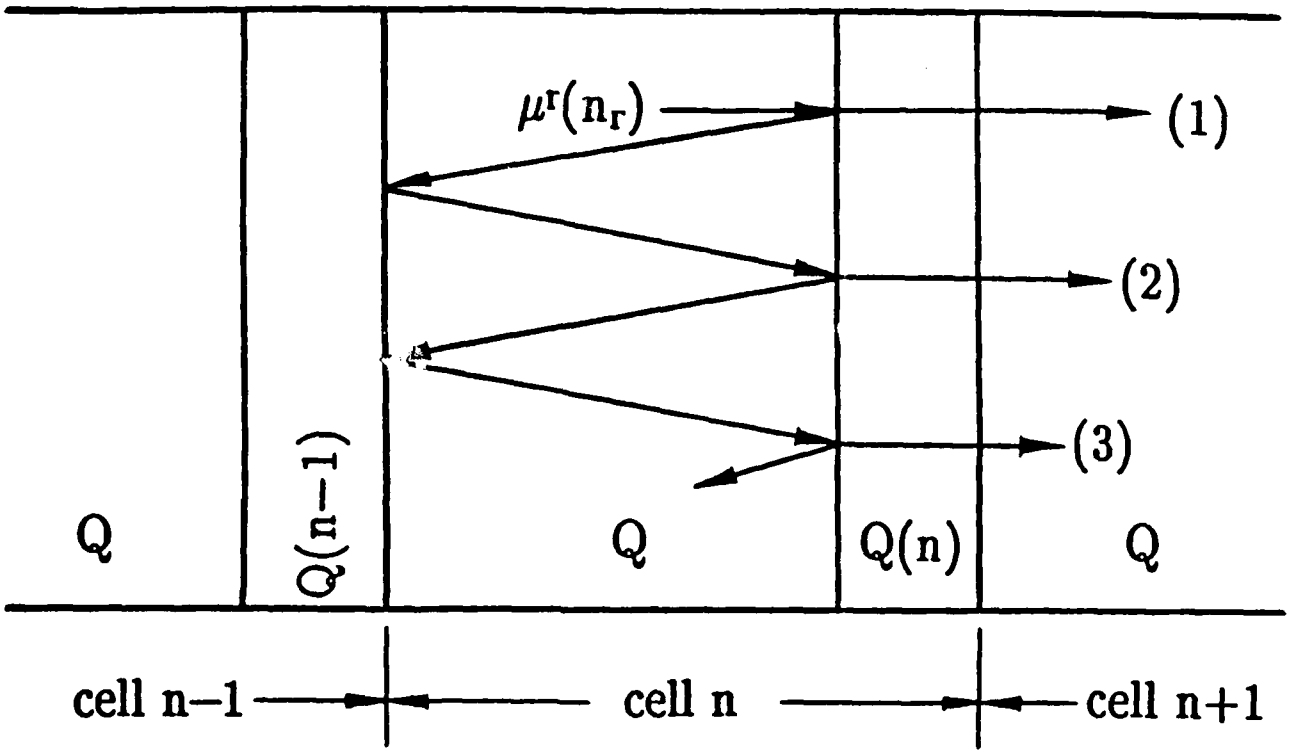

(1) $t(n)\mu^r(n_r)$

(2) $t(n)\lambda^2 r^\ell(n-1)r^r(n)\mu^r(n_r)$

(3) $t(n)[\lambda^2 r^\ell(n-1)r^r(n)]^2\mu^r(n_r)$

Fig. 3 Schematic representation of transmitted waves through the interface between cells n and n+1

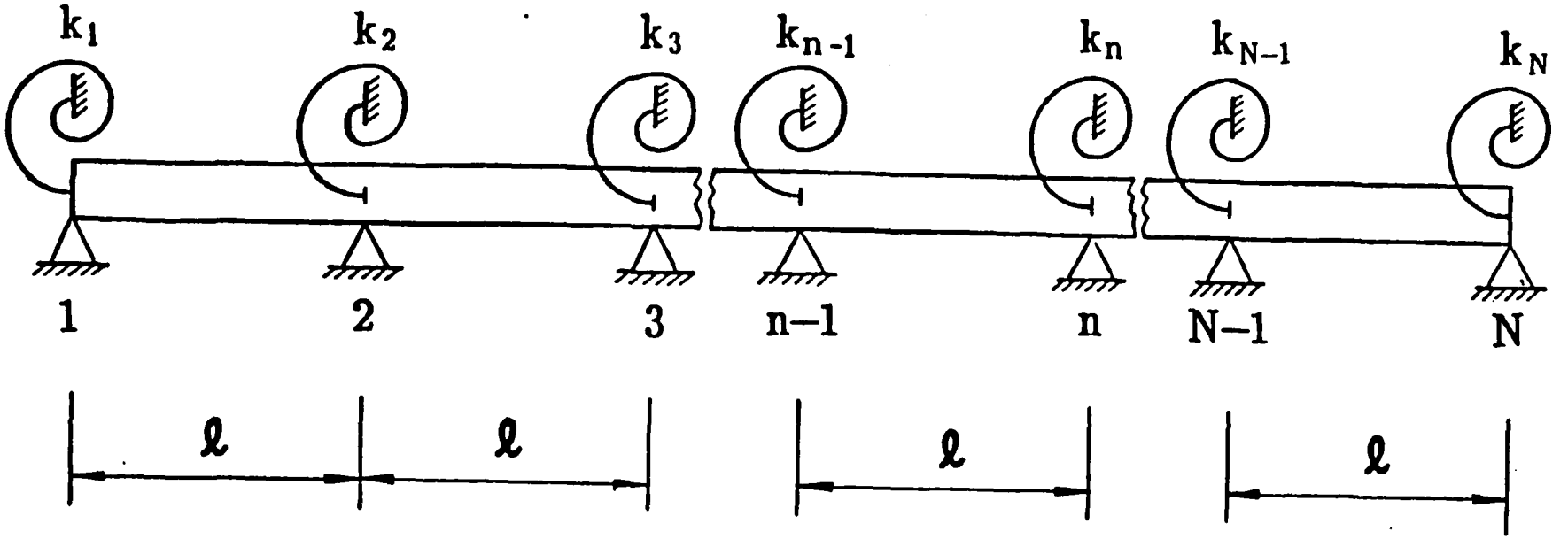

Fig. 4 A beam on hinge supports with additional torsional spring at each support

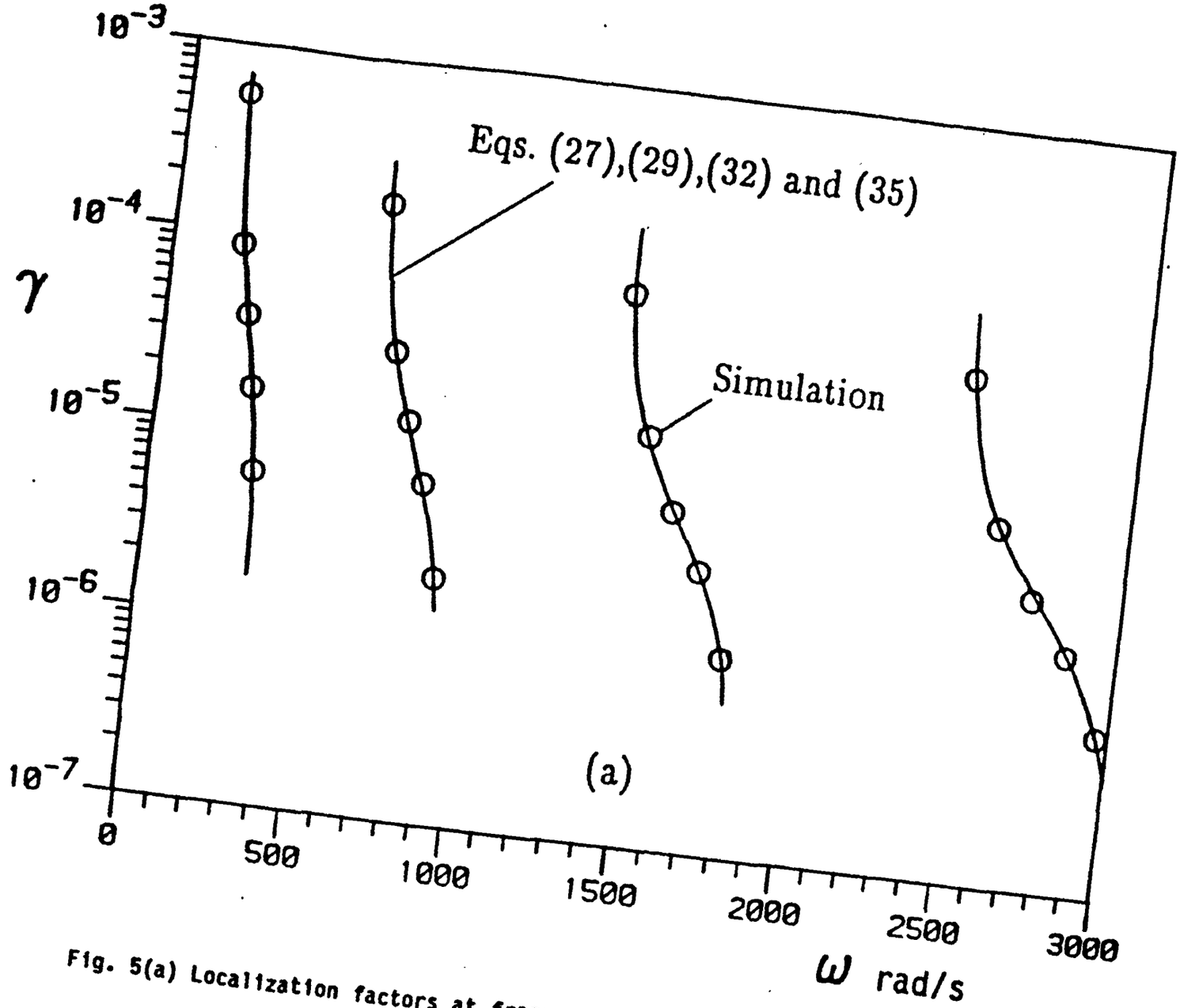

Fig. 5(a) Localization factors at frequencies in wave-passage frequency bands 1 through 4; $\delta = 1$, $\sigma = 0.1$

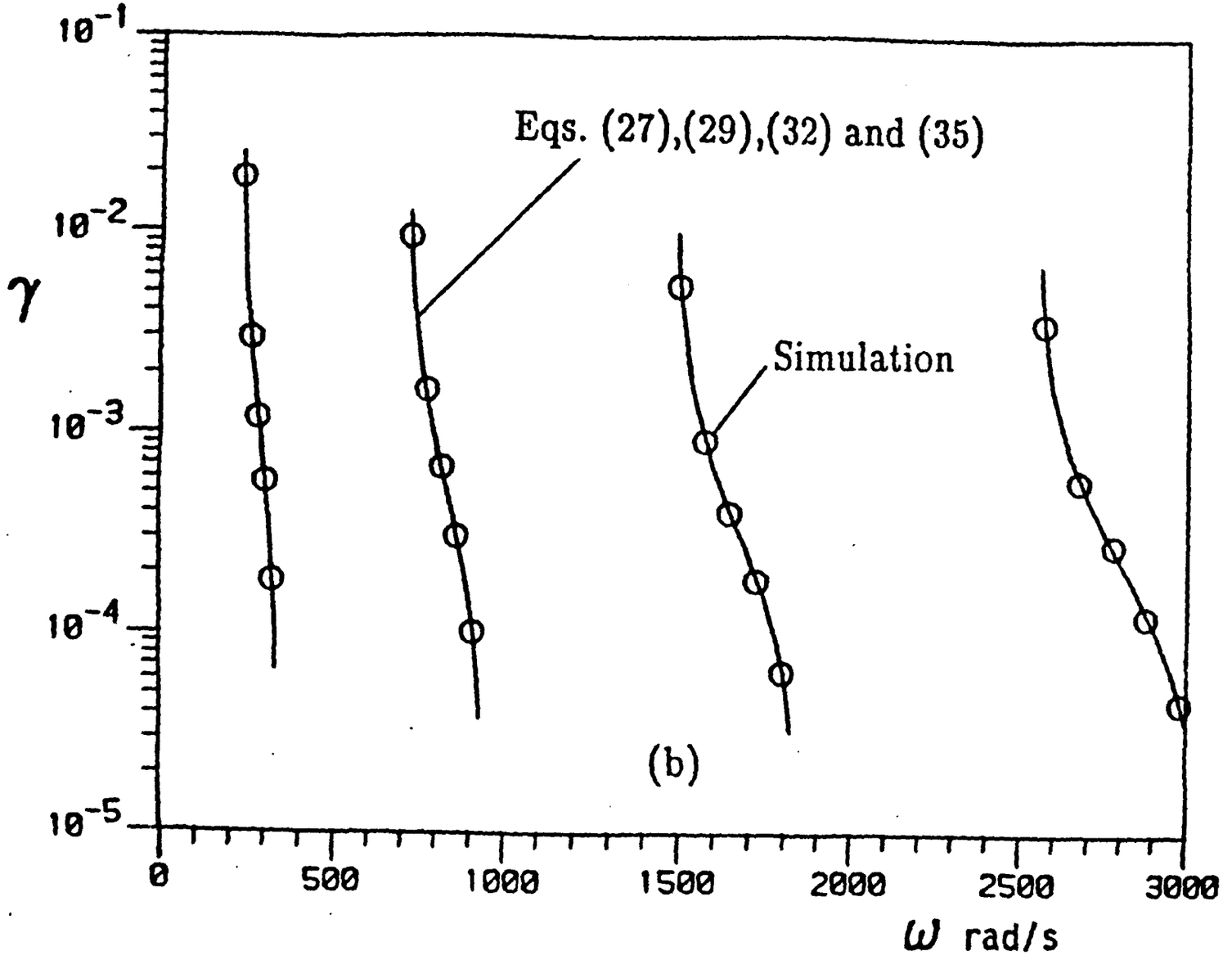

Fig. 5(b) Localization factors at frequencies in wave-passage frequency bands 1 through 4; $\delta = 0.1$, $\sigma = 0.1$

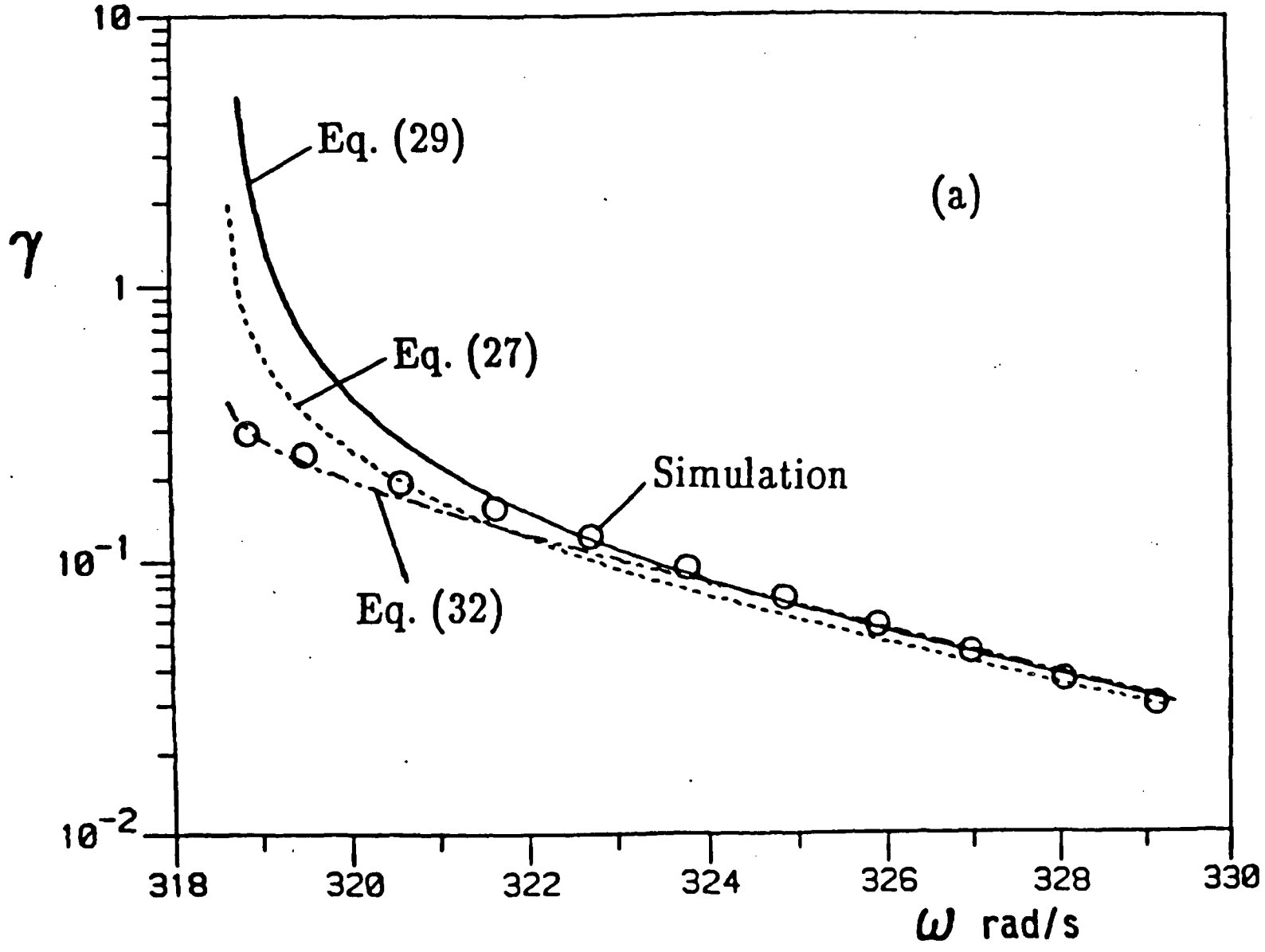

Fig. 6(a) Localization factors at frequencies in the lower half of the first wave-passage frequency band; $\delta = 0.01$, $\sigma = 0.25$

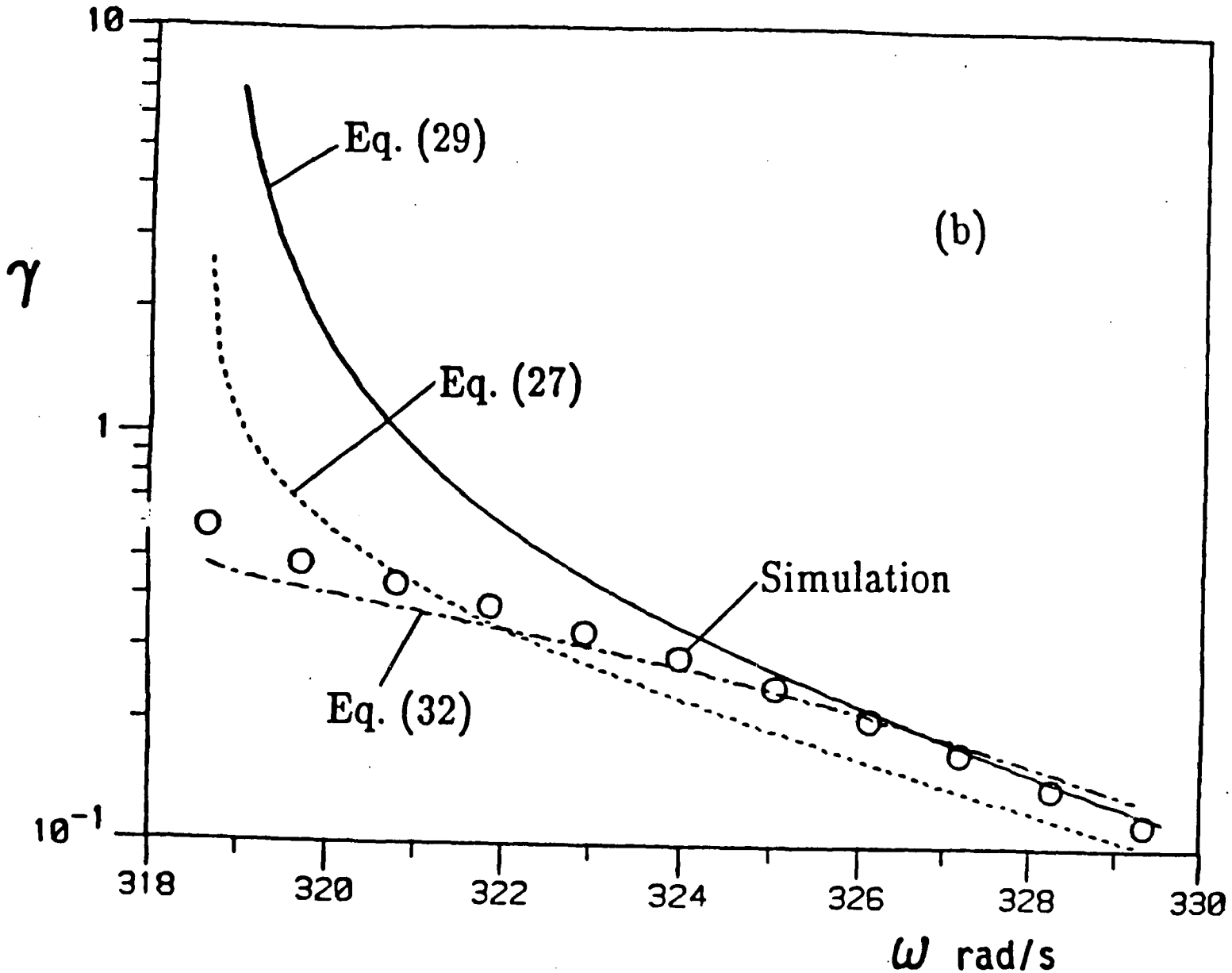

Fig. 6(b) Localization factors at frequencies in the lower half of the first wave-passage frequency band; $\delta = 0.01$, $\sigma = 0.5$

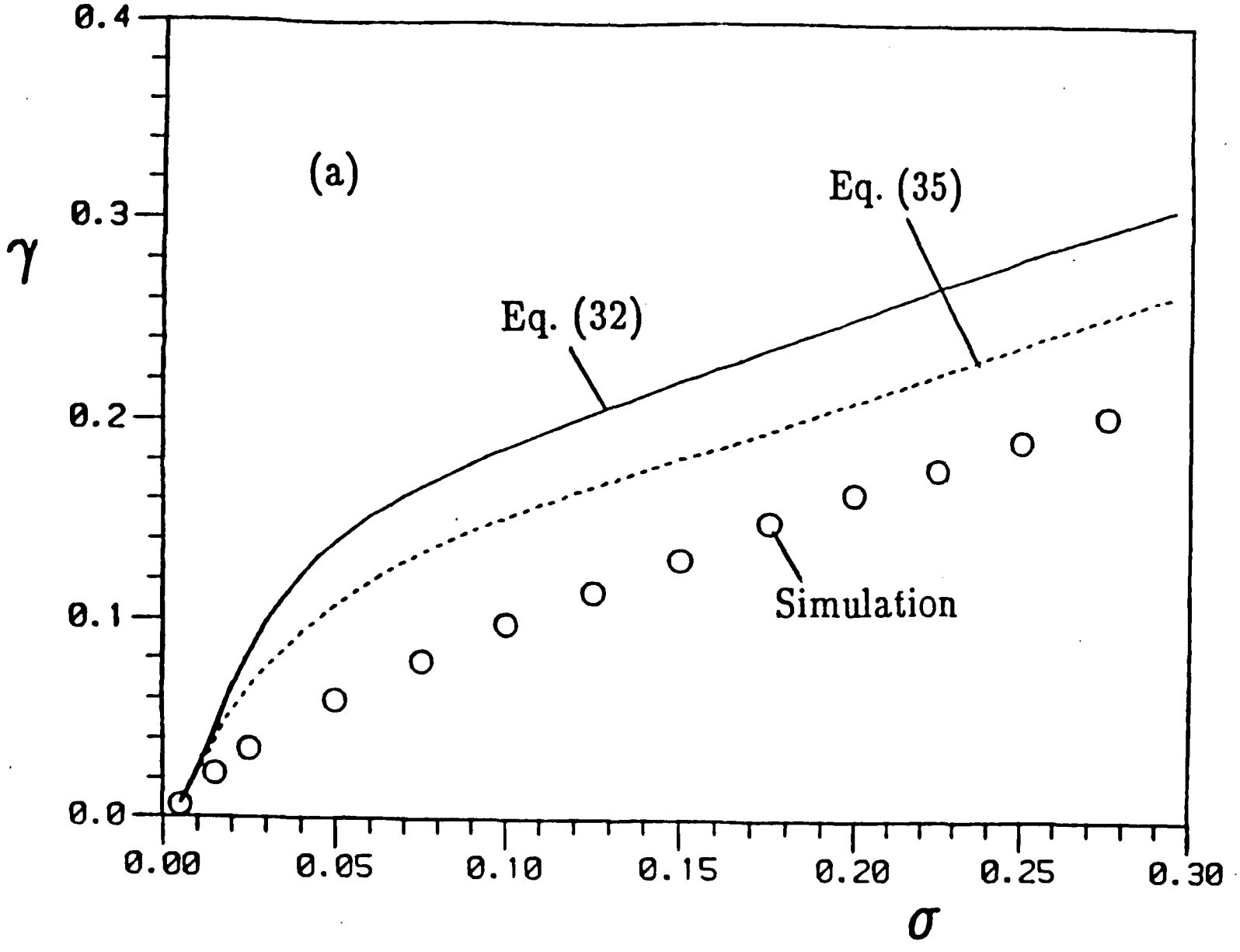

Fig. 7(a) Localization factors at frequencies near the lower boundaries of the first wave-passage frequency band; $\delta = 0.1$, $\omega = 232.5$ rad/s

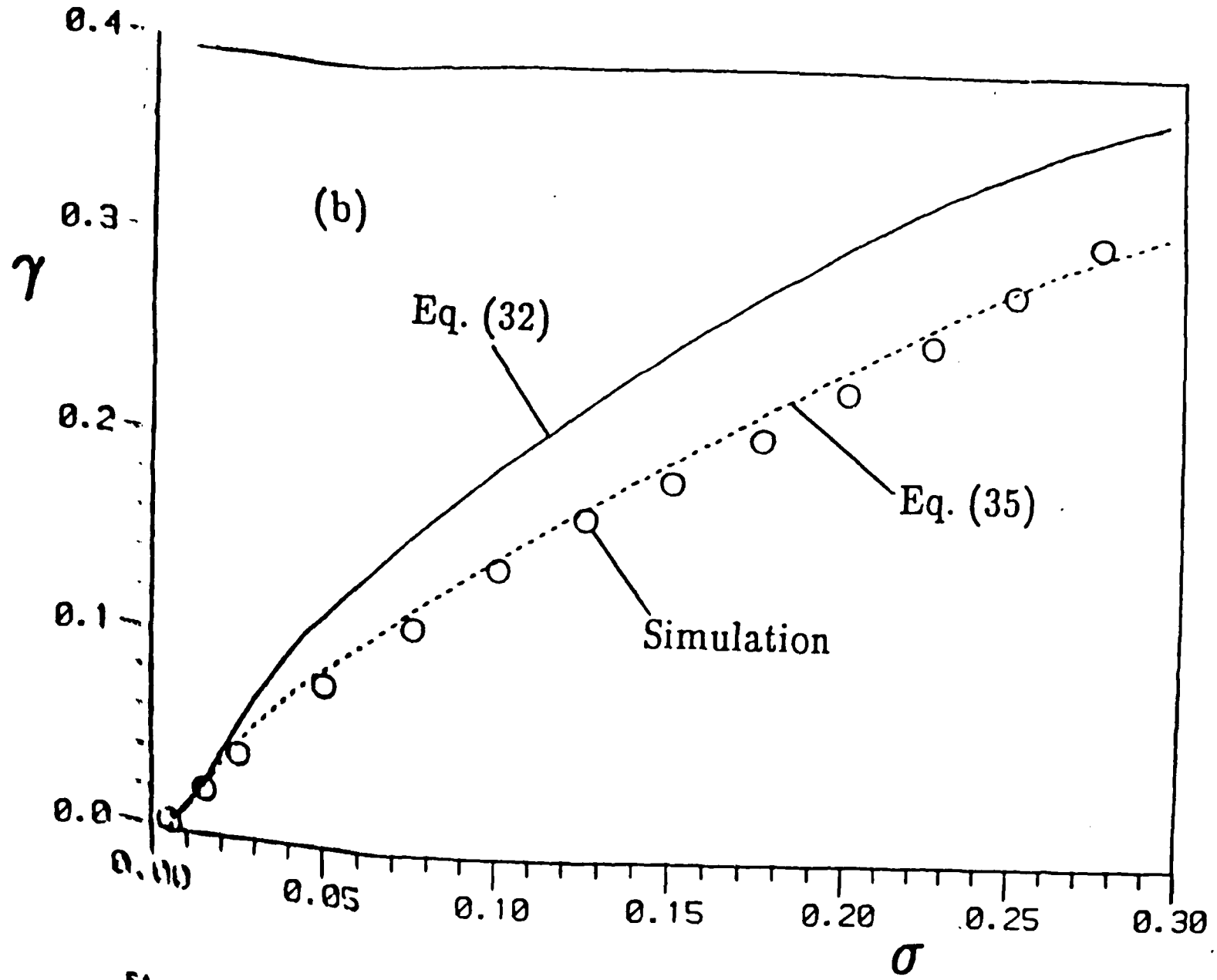

Fig. 7(b) Localization factors at frequencies near the lower boundaries of the first wave-passage frequency band; $\delta = 0.01$, $\omega = 318.7$ rad/s

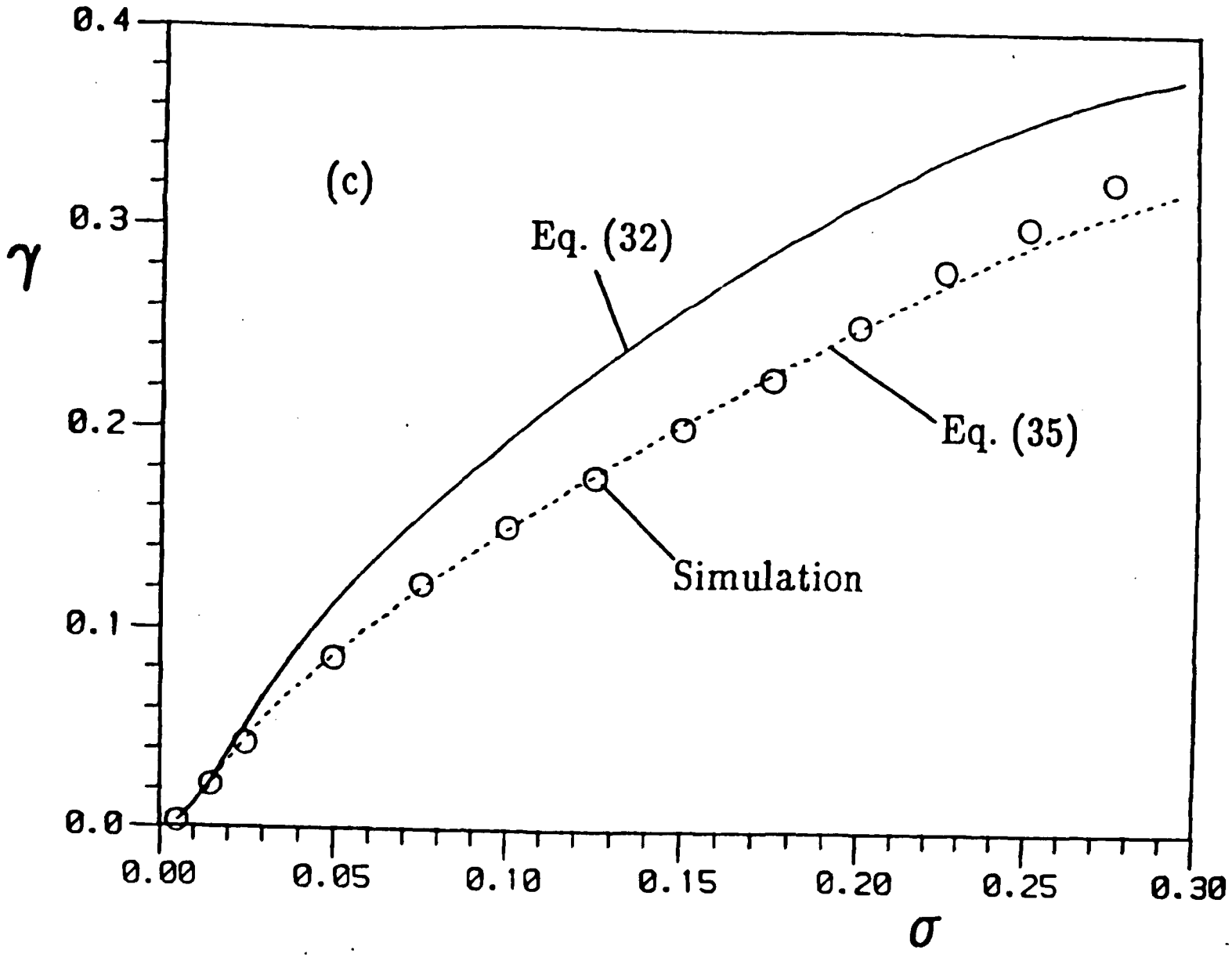

Fig. 7(c) Localization factors at frequencies near the lower boundaries of the first wave-passage frequency band; $\delta = 0.001$, $\omega = 339.72$ rad/s

EXACT AND APPROXIMATE SOLUTION TECHNIQUES IN NON-LINEAR RANDOM VIBRATION

Consider a dynamical system governed by

$$\frac{d}{dt} X_j = f_j(X,t) + g_{jk}(X,t)F_k(t);$$
$$j = 1,2,\ldots,N; \qquad k = 1,2,\ldots,M \tag{1}$$

in which t is the time variable, X_j are components of the system response vector X, $F_k(t)$ are random processes representing the random excitations, and a repeated subscript in a product indicates a summation. Functions f_j and g_{jk} are generally nonlinear; however, their functional forms are deterministic.

Two types of random excitation are possible. A particular $F_k(t)$ is a multiplicative (or parametric) excitation if its accompanying factor $g_{jk}(X,t)$ depends explicitly on the response X; it is an additive (or external) excitation if its accompanying factor does not depend on X. In other words, a multiplicative excitation appears as the coefficient of an unknown in the governing equations whereas an additive excitation appears as an inhomogeneous term. The roles played by the two types of random excitations are fundamentally different.

Exact Solutions

Exact solutions for randomly excited nonlinear systems are difficult to obtain. The possibility for exact solutions exists if the random excitations can be idealized as Gaussian white noises. In such a case the response of a system to random excitations, represented as a vector in a state space, is a Markov vector. The probability density of a Markov vector, conditional on the knowledge of the initial state, is governed by a parabolic partial differential equation, called the Fokker-Planck equation, which can be derived from the equations of motion. Still, exact solutions for the Fokker-Planck equation is known only for very special first order nonlinear systems, which are of little

interest to structural engineers. For higher order systems, solutions have been obtained for the reduced Fokker-Planck equations; namely, Fokker-Planck equations without the time derivative term. The unknown in a reduced Fokker-Planck equation is the unconditional probability density of the system response when it reaches the state of statistical stationarity. This can occur if the f_j and g_{jk} functions in equation (1) do not depend explicitly on t, and if energy can be dissipated from the system to balance the input energy from the excitations.

The Fokker-Planck equation has the general form of

$$\frac{\partial}{\partial t} q + \frac{\partial}{\partial x_j} G_j = 0 \tag{2}$$

where q is an abbreviated symbol for the unknown conditional probability density $q_X(x,t|\, x_o,t_o)$, and G_j is the probability flow in the jth direction given by

$$G_j = A_j(x)q - \frac{1}{2}\frac{\partial}{\partial x_k}[B_{jk}(x)q] \tag{3}$$

In (2) and (3), a lower case symbol represents the possible value of a random quantity. For example, x is a possible value of X, x_j a possible value of X_j, etc. This convention will be followed throughout the paper. In equation (3) A_j and B_{jk} are called the first and second derivate moments (also known as the drift and diffusion coefficients), respectively, which can be obtained from the equations of motion as follows using the well-known rules of Wong and Zakai [1]:

$$A_j(x) = f_j(x) + \pi K_{\ell s}\, g_{rs} \frac{\partial}{\partial x_r} g_{j\ell}(x) \tag{4}$$

$$B_{jk}(x) = 2\pi K_{\ell s}\, g_{j\ell}\, g_{ks} \tag{5}$$

In (4) and (5) each $K_{\ell s}$ is a constant, representing the joint spectral density of $F_\ell(t)$ and $F_s(t)$, which are now restricted to be Gaussian white noises so that an exact probabilistic solution can be obtained. $K_{\ell s}$ is related to the cross-correlation function of $F_\ell(t)$ and $F_s(t)$ as

$$E[F_\ell(t_1)F_S(t_2)] = 2\pi K_{\ell S}\,\delta(t_1 - t_2) \tag{6}$$

An exact solution, if obtainable, must satisfy the initial condition

$$q_X(x,t_o|\,x_o,t) = \prod_{j=1}^{N}\delta(x_j - x_{j,o}) \tag{7}$$

and appropriate boundary conditions. If the total probability measure must be preserved, then the boundary conditions must be natural, namely,

$$G_j = 0 \quad \text{at the boundaries} \tag{8}$$

We shall be interested in the stationary state solutions, governed by the reduced Fokker-Planck equation

$$\frac{\partial}{\partial x_j} G_j = 0 \tag{9}$$

$$G_j = A_j(x)p_S(x) - \frac{1}{2}\frac{\partial}{\partial x_k}\left[B_{jk}(x)p_S(x)\right] \tag{10}$$

where $p_S(x)$ is the stationary probability density of X independent of t. Equation (9) is solved with the boundary conditions (8).

1. The Case of Stationary Potential

The special case of stationary potential considered by Stratonovich [2] is one in which the probability flow vanishes everywhere not only at the boundaries, namely

$$A_j(x)p_S(x) - \frac{1}{2}\frac{\partial}{\partial x_k}\left[B_{jk}(x)p_S(x)\right] = 0 \tag{11}$$

Without loss of generality, write the solution for (11) as

$$p_S(x) = C\exp(-\phi) \tag{12}$$

This solution form guarantees that the probability density, if it exists, is non-negative for a positive normalization constant C. Substituting (12) into (11), one obtains

$$B_{jk}\frac{\partial\phi}{\partial x_k} = \frac{\partial}{\partial x_k}B_{jk} - 2A_j \tag{13}$$

These are N equations for ϕ. If a consistent ϕ function can be obtained from (13), then the stochastic system belongs to the class of stationary potential.

For a first order system, for which the state space is one-dimensional, namely N = 1, the probability flow must vanish everywhere if it vanishes at the boundaries. Then (13) reduces to

$$B \frac{d\phi}{dx} = \frac{d}{dx} B - 2A \tag{14}$$

Solving for ϕ

$$\phi = \ell nB - 2 \int AB^{-1} \, dx \tag{15}$$

Unfortunately, as to be explained later, oscillatory dynamic systems do not belong to the class of stationary potential. Since structural systems are usually oscillatory a more general procedure is needed and will be discussed in the next section.

2 The Case of Generalized Stationary Potential

Circulatory probability flows are generally present in a multi-dimensional state space. To provide for additional flexibility in obtaining a solution to equation (9), we split the drift and diffusion coefficients as follows [3,4]

$$A_j = A_j^{(1)} + A_j^{(2)} \tag{16}$$

$$B_{jk} = B_{jk}^{(j)} + B_{kj}^{(k)} \tag{17}$$

Equation (17) retains the symmetry condition for diffusion coefficients; i.e. $B_{jk} = B_{kj}$. Substituting (16) and (17) into (9), one obtains

$$\frac{\partial}{\partial x_j} \left[A_j^{(1)} p_s - \frac{\partial}{\partial x_k} B_{jk}^{(j)} p_s \right] + \frac{\partial}{\partial x_j} [A_j^{(2)} p_s] = 0 \tag{18}$$

Let $A_j^{(1)}$ be associated with the vanishing probability flow, and $A_j^{(2)}$ associated with the circulatory probability flow. Then for p_s expressed in the form of (12), it can be shown that

$$\frac{\partial}{\partial x_j} A_j^{(2)} = A_j^{(2)} \frac{\partial \phi}{\partial x_j} \tag{19}$$

$$A_j^{(1)} = \frac{\partial}{\partial x_k} B_{jk}^{(j)} - B_{jk}^{(j)} \frac{\partial \phi}{\partial x_k} \tag{20}$$

The superscript (j) in (20) does not imply a summation. There are a total of n + 1 equations for ϕ in the set of (19) and (20). The problem is solvable if a consistent ϕ function can be obtained from these equations. Such a solvable problem is said to belong to the case of generalized stationary potential [3,4]. It is of interest to note that if the system is in a state known as detailed balance [e.g. 5,6], then the two parts of each drift coefficient $A_j^{(1)}$ and $A_j^{(2)}$ correspond to the so-called irreversible and reversible parts, respectively. However, (19) and (20) are more general, and are applicable to systems not in detailed balance.

3 Applications

The above solution technique will now be applied to single-degree-of-freedom second order systems of the type

$$\ddot{Z} + \psi(Z,\dot{Z}) = \theta_k(Z,\dot{Z})W_k(t) \tag{21}$$

where $W_k(t)$ are Gaussian white noises with delta type correlations; i.e.

$$E[W_k(t)W_\ell(t+\tau)] = 2\pi K_{k\ell}\,\delta(\tau) \tag{22}$$

Equation (21) is equivalent to two first order equations in the form of (1)

$$\frac{d}{dt}X_1 = X_2 \tag{23}$$

$$\frac{d}{dt}X_2 = -\psi(X_1,X_2) + \theta_k(X_1,X_2)\,W_k(t)$$

It follows from (4) and (5) that

$$A_1 = x_2,$$

$$A_2 = -\psi(x_1,x_2) + \pi K_{k\ell}\,\theta_\ell(x_1,x_2)\frac{\partial}{\partial x_2}\theta_k(x_1,x_2)$$

$$B_{11} = B_{12} = B_{21} = 0, \qquad B_{22} = 2\pi K_{k\ell}\theta_k(x_1,x_2)\theta_\ell(x_1,x_2)$$

Split the drift and diffusion coefficients into

$$A_1^{(1)} = 0, \qquad A_1^{(2)} = x_2$$

$$A_2^{(1)} = -\psi(x_1,x_2) + \pi K_{k\ell}\,\theta_\ell\,\frac{\partial}{\partial x_2}\,\theta_k + \lambda_x/\lambda_y$$

$$A_2^{(2)} = -\lambda_x/\lambda_y, \qquad B_{22}^{(2)} = \frac{1}{2} B_{22}, \qquad B_{12}^{(1)} = -B_{21}^{(2)}$$

where λ is an arbitrary function of $x = x_1$ and $y = \frac{1}{2}x_2^2$, and is twice differentiable with respect to its arguments. The physical meaning of λ will be discussed later. Then application of (19) and (20) results in

$$-x_2 \frac{\partial \phi}{\partial x_1} + (\lambda_x/\lambda_y) \frac{\partial \phi}{\partial x_2} - \frac{\partial}{\partial x_2} (\lambda_x/\lambda_y) = 0 \tag{24}$$

$$B_{12}^{(1)} \frac{\partial \phi}{\partial x_2} = \frac{\partial}{\partial x_2} B_{12}^{(1)} \tag{25}$$

$$B_{21}^{(2)} \frac{\partial \phi}{\partial x_1} + \pi K_{k\ell}\, \theta_k\, \theta_\ell \frac{\partial \phi}{\partial x_2} = \frac{\partial}{\partial x_1} B_{21}^{(2)} + \psi(x_1, x_2) + \pi K_{k\ell}\, \theta_k \frac{\partial}{\partial x_2} \theta_\ell - \lambda_x/\lambda_y \tag{26}$$

The general solution of (24) is

$$\phi(x_1, x_2) = -\ell n\, \lambda_y + \phi_0(\lambda) \tag{27}$$

where $\phi_0(\lambda)$ is an arbitrary function of λ. In order that (25) and (26) can also be satisfied, the ψ and θ_k functions must be related as

$$\psi(x_1, x_2) = \pi x_2 K_{k\ell}\, \theta_k\, \theta_\ell \left[\lambda_y\, \phi_0'(\lambda) - \lambda_{yy}/\lambda_y\right] - \pi K_{k\ell}\, \theta_\ell \frac{\partial}{\partial x_2} \theta_k + \lambda_x/\lambda_y + D(x_1)\, e^{\phi_0(\lambda)}/\lambda_y \tag{28}$$

where $D(x_1)$ is an arbitrary function of x_1 alone. Equation (28) provides a restriction between the constitutive law of the system, as represented by ψ and θ_k on one hand, and the spectral densities $K_{k\ell}$ on the other, so that the exact solution for the stationary probability density is obtainable using the present procedure.

The well-known case [7,8] of linear damping, nonlinear spring, and an additive Gaussian white noise excitation

$$\ddot{Z} + \beta \dot{Z} + g(Z) = W(t), \qquad \beta > 0 \tag{29}$$

corresponds to a single $\theta = 1$ and

$$\psi(x_1, x_2) = \beta x_2 + g(x_1) \tag{30}$$

Then letting $D(x_1) = 0$ and

$$\lambda = y + \int_0^x g(u)du = \frac{1}{2}x_2^2 + \int_0^{x_1} g(u)du \tag{31}$$

equation (28) reduces to

$$\phi_0'(\lambda) = \frac{\beta}{\pi K} \tag{32}$$

where K is the spectrum of the white noise. Furthermore, $\phi(\lambda) = \phi_0(\lambda)$ in this case. Thus

$$p_S(x_1,x_2) = C \exp(-\frac{\beta}{\pi K}\lambda)$$

$$= C \exp\{-\frac{\beta}{\pi K}[\frac{1}{2}x_2^2 + \int_0^{x_1} g(u)du]\} \tag{33}$$

which is a valid probability density if λ is positive for large $|x_1|$.

Without specifying the form for the λ function, but still letting $D(x_1) = 0$ and restricting to a single additive excitation, one obtains from (28)

$$\phi_0'(\lambda) = \frac{\psi(x_1,x_2) - \lambda_x/\lambda_y + \pi K x_2(\lambda_{yy}/\lambda_y)}{\pi K x_2 \lambda_y} \tag{34}$$

Note that the right hand side of (34) must be a function of λ alone. If this is satisfied, then (34) can be used to obtain the required $\phi_0(\lambda)$.

The solution obtained by Caughey and Ma [9] corresponds to

$$\psi(x_1,x_2) = \lambda_x/\lambda_y + \pi K x_2 [\lambda_y h(\lambda) - \lambda_{yy}/\lambda_y] \tag{35}$$

where h( ) is an arbitrary function subject to a rather general restriction to be specified later. Substitution of (35) into (34) results in

$$\phi_0'(\lambda) = h(\lambda) \tag{36}$$

and a stationary probability density

$$p_S(x_1,x_2) = C\lambda_y \exp[-\int_0^{\lambda} h(\nu)d\nu] \tag{37}$$

The λ and h functions must be such that the right hand side of (37) is normalizable. This extremely simple result is obtained under a rather

artificial assumption that the constitutive law of the system itself, namely $\psi(x_1,x_2)$ is dependent on the spectrum K of the excitation.

The physical meaning of the λ function can be revealed by considering the deterministic case of undamped free motion governed by

$$\ddot{x} + \lambda_x/\lambda_y = 0 \tag{38}$$

Since $\ddot{x} = (1/2)(d\dot{x}^2/dx) = dy/dx$, the above equation can be replaced by

$$d\lambda = \lambda_x dx + \lambda_y dy = 0 \tag{39}$$

Therefore, $\lambda(x,y)$ is not truly arbitrary; it represents the total energy in the conservative system (38). It should be noted, however, that this physical interpretation must be modified if multiplicative random excitation appears in the coefficient of the first derivative term in a second order differential equation.

Equations (19) and (20) have been applied to obtain new solutions for systems under both additive and multiplicative excitations [4,10]. The following two examples will illustrate some of the possibilities.

The first example is described by

$$\ddot{Z} + [\alpha + \frac{\beta}{2}(\dot{Z} + \omega_0^2 Z)^2 + W_2(t)]\dot{Z} + \omega_0^2 [1 + W_1(t)]Z = W_3(t) \tag{40}$$

where $W_1(t)$, $W_2(t)$ and $W_3(t)$ are independent Gaussian white noises with spectra K_{11}, K_{22} and K_{33}, respectively. Under the restriction $\omega_0^4 K_{11}=K_{22}$ the stationary probability density for $Z=X_1$ and $Z=X_2$ is given by [14]

$$p_S(x_1,x_2) = C(\lambda + \frac{K_{33}}{2K_{22}})^{-\gamma} \exp(-\frac{\beta}{2\pi K_{22}}\lambda) \tag{41}$$

where $\gamma = \frac{1}{2}(\frac{\alpha}{\pi K_{22}} + 1 - \frac{\beta}{\pi K_{22}^2} K_{33})$ and $\lambda = \frac{1}{2} x_2^2 + \frac{1}{2} \omega_0^2 x_1^2$

Equation (41) is a generalization of a result obtained previously by Dimentberg [10] for the special case $K_{33} = 0$, namely, when the additive random excitation

is absent, in which case, the value for γ is restricted to $\gamma < 1$; otherwise, the right hand side of (41) is not normalizable. This can occur, of course, only if $\alpha < 0$ and $K_{22} > |\alpha|/\pi$. It means that the trivial solution $Z=\dot{Z}=0$ is unstable in probability when $K_{22} > |\alpha|\pi$.

The second example is an interesting nonlinear oscillator capable of exhibiting limit cycle and bifurcation behaviors, governed by [11].

$$\ddot{Z} + Z^2[\beta + \frac{4\alpha}{Z^2+\dot{Z}^2}]\ \dot{Z} + [1 + W(t)]\ Z = 0 \qquad (42)$$

where $\beta > 0$, and $W(t)$ is a Gaussian white noise multiplicative excitation with a spectral density K. Without the random excitation, the equation has a non-trivial solution, corresponding to a stable limit-cycle if $\alpha < 0$. If $\alpha > 0$, then the only stable configuration is the trivial $Z = 0$.

The stationary probability density for $Z=X_1$ and $\dot{Z}=X_2$ is found to be

$$p_S(x_1,x_2) = C(x_1^2 + x_2^2)(2\alpha/\pi K)\ \exp[-\frac{\beta}{2\pi K}(x_1^2 + x_2^2)] \qquad (43)$$

Equation (43) implies that if $\alpha > 0$ then a nontrivial stationary probability density exists only if $K > 2\alpha/\pi$. Thus, $2\alpha/\pi$ represents a critical spectral level for the multiplicative excitation at which bifurcation occurs, and below which the trivial solution is stable in probability. When a stationary probability density of the system response exists ($K > 2\alpha/\pi$), its shape depends on whether $\alpha \geq 0$ or $\alpha < 0$. It can be shown that if $\alpha \geq 0$, then the probability density p_S has a peak at $x_1 = x_2 = 0$. On the other hand, if $\alpha < 0$, then p_S has a maximum at $x_1^2 + x_2^2 = 4|\alpha|/\beta$ and it tends to zero as $x_1^2 + x_2^2$ approaches to either zero or infinity. This implies that the probability density has a shape shown in Fig. 1, and the most probable values for the response lie on the circle $x_1 + x_2 = 4|\alpha|/\beta$, which is the stochastic analogue of the limit cycle.

To the knowledge of the writer, the class of generalized stationary

potential, satisfying (19) and (20), includes all the stochastic systems whose exact probability solution in the stationary state are known to date. When both multiplicative and additive random excitations are present, restriction on the system parameters and excitation spectral levels are generally required to obtain such solutions.

Approximate Solutions

When both multiplicative and additive random excitations are present, restrictions usually must be imposed on the relationship between the noise spectra and some system parameters in order to obtain an exact stationary-state solution for the response of a nonlinear system at the present time. In practical engineering applications, the excitation spectral levels cannot be so restricted; therefore, approximate procedures are often needed to obtain the solutions.

1 Cumulant-Neglect Closure

One versatile scheme to obtain approximate solutions is the cumulant-neglect closure [14,15] which can be applied easily if random excitations are Gaussian white noises or filtered Gaussian white noises. Return to (1) and convert these equations to the Itô type stochastic differential equations as follows [e.g. 16]

$$dX_j(t) = m_j(X,t)dt + \sigma_{j\ell}(X,t)dB_\ell(t) \tag{44}$$

where $B_\ell(t)$ are independent unit Wiener processes, and

$$m_j(X,t) = A_j(X,t) \tag{45}$$

$$\sigma_{j\ell}(X,t)\,\sigma_{k\ell}(X,t) = B_{jk}(X,t) \tag{46}$$

The right hand sides of (45) and (46) are the same drift and diffusion coefficients in (4) and (5), but with x replaced by X. However, these

coefficients can now depend on t, and the results in this section are not restricted to the stationary response. One can then obtain equations for the statistical moments for X(t) by using Itô's differential rule [17]

$$\frac{d}{dt} E[F(X,t)] = E[\frac{\partial F}{\partial t} + (m_j \frac{\partial F}{\partial X_j} + \frac{1}{2} \sigma_{j\ell}\sigma_{k\ell} \frac{\partial^2 F}{\partial X_j \partial X_k})] \qquad (47)$$

and by letting F be X_i, X_iX_r, $X_iX_rX_s$, etc. For nonlinear systems, the equations for statistical moments form an infinite hierarchy, and they can only be solved approximately using a suitable closure scheme.

The statistical moments are related to cumulants as follows [2,18]:

$$\begin{aligned}
E[X_j] &= \kappa_1[X_j] \\
E[X_jX_k] &= \kappa_2[X_j,X_k] + \kappa_1[X_j]\kappa_1[X_k] \\
E[X_jX_kX_\ell] &= \kappa_3[X_j,X_k,X_\ell] + 3\{\kappa_1[X_j]\kappa_2[X_k,X_\ell]\}_S \\
&\quad + \kappa_1[X_j]\kappa_1[X_k]\kappa_1[X_\ell] \\
E[X_jX_kX_\ell X_m] &= \kappa_4[X_j,X_k,X_\ell,X_m] + 3\{\kappa_2[X_j,X_k]\kappa_2[X_\ell,X_m]\}_S \\
&\quad + 4\{\kappa_1[X_j]\kappa_3[X_k,X_\ell,X_m]\}_S + 6\{\kappa_1[X_j]\kappa_1[X_k]\kappa_2[X_\ell,X_m]\}_S \\
&\quad + \kappa_1[X_j]\kappa_1[X_k]\kappa_1[X_\ell]\kappa_1[X_m] \\
&\quad \cdots\cdots\cdots\cdots
\end{aligned} \qquad (48)$$

where $\kappa_j[\ ]$ denotes a jth cumulant, and $\{\ \}_S$ indicates a symmetrizing operation with respect to its arguments; namely, taking the arithmetic mean of <u>different</u> permuted terms similar to the one within the braces. In a cumulant-neglect closure, all the cumulants higher than a given order N are set to zero. The statistical moments of an order higher than N can then be expressed in terms of lower order moments using (48). Very accurate results have been obtained using this scheme [14] as long as the spectral levels of multiplicative random excitations are not too high so that the system is far from stochastic

bifurcation or instability [19,20].

It is of interest to note that for a random process defined on $(-\infty, \infty)$, neglecting κ_n for $n > 2$ is equivalent to the so-called Gaussian closure; namely, approximating this random process by a Gaussian process. Gaussian closure, however, is the simplest and of the lowest order among non-trivial cumulant-neglect closures. Furthermore, if the excitations are white noises or filtered white noises, then Gaussian closure leads to the same results as statistical equivalent linearization. A review of recent contributions to the equivalent linearization schemes has been given by Spanos [21]. Another closure scheme, using a truncated Gram-Charlier or Edgeworth series [22,23] has a similar accuracy as that of cumulant closure; however, it is more difficult to apply to multi-degree-of-freedom systems when a multidimensional Gram-Charlier series is required.

2 Generalized Equivalent Linearization

The development of generalized equivalent linearization scheme by Brückner and Lin [24] was motivated by two reasons: (1) a cumulant-neglect closure of an order N>2 does not guarantee a non-negative probability density everywhere, (2) the traditional equivalent linearization, which leads to the same result as that of Gaussian closure, replaces the original nonlinear system with a linear system devoid of parametric excitation; therefore, it is unsuitable to treat the case when random parametric excitations are also present.

In a generalized equivalent linearization scheme, the original Itô system, (44) is replaced by a linear Itô system as follows:

$$dX_j(t) = (a_{jk}X_k + b_j)dt + (c_{jrs}X_r + d_{js})dB_s(t) \qquad (49)$$

The equations for the first and second order statistical moments are closed; they may be determined from

$$\frac{d}{dt} E[X_j] = a_{jk} E[X_k] + b_j \tag{50}$$

$$\begin{aligned}\frac{d}{dt} E[X_j X_r] &= a_{rs} E[X_j X_s] + a_{jk} E[X_r X_k] \\ &+ c_{jk\ell} c_{rp\ell} E[X_k X_p] + b_r E[X_j] + b_j E[X_r] \\ &+ c_{jk\ell} d_{r\ell} E[X_k] + c_{rp\ell} d_{j\ell} E[X_p] + d_{j\ell} d_{r\ell}\end{aligned} \tag{51}$$

The constants a_{jk}, b_j, c_{jrs} and d_{js} are determined by minimizing the mean-square errors

$$\epsilon_j = E\{[m_j(X) - a_{jk}X_k - b_j]^2\} \tag{52}$$

$$\begin{aligned}\epsilon_{jr} = E\{[&X_j m_r(X) + X_r m_j(X) + \sigma_{j\ell}(X)\,\sigma_{r\ell}(X) - a_{rs}X_j X_s \\ &- a_{jk}X_r X_k - C_{jk\ell}\,c_{rp\ell}\,X_k X_p - b_r X_j - b_j X_r \\ &- c_{jk\ell}\,d_{r\ell}\,X_k - c_{rp\ell}\,d_{j\ell}\,X_p - d_{j\ell}\,d_{r\ell}]^2\}\end{aligned} \tag{53}$$

To carry out the minimization process, the evaluation of certain moments higher than the second order is still required. However, when the optimal constants so obtained are substituted into Eq.(49), the linearized system does possess a non-negative probability density.

3 Stochastic Averaging

Method of stochastic averaging was developed by Stratonovich [2] based primarily on physical arguments. It was later justified and interpreted rigorously by Khasminskii [25], Papanicolaous and Kohler [26]. The first application to structural systems was due to Ariaratnam in the anlaysis of column stability under random axial load [27]. Lin and coworkers have used the procedure to investigate the effects of atmospheric turbulence on the motions of helicopter blades [e.g. 28,29,30,31], and of long-span bridges [32,33]. Namachichivaya and Ariaratnam [34] and Namachchivaya [35,36] applied the method to Hopf bifurcation in the presence of stochastic excitations. A review of the general subject and many other contributions was given by Roberts and Spanos

[37].

According to Stratonovich [2] the response of a dynamic system to random excitation may be approximated by a Markov vector, if the correlation times of all the excitations are short compared with the relaxation time of the system. Then the coefficients in the corresponding Itô type differential equations (44) can be obtained from the original physical equations (1) as follows:

$$m_j = f_j(X,t) + \int_{-\infty}^{0} \frac{\partial}{\partial X_\ell} g_{jk}(X,t)\, g_{\ell s}(X,t+\tau)\, E[F_k(t)\, F_s(t+\tau)]d\tau \tag{54}$$

$$\sigma_{j\ell}\, \sigma_{k\ell} = \int_{-\infty}^{\infty} g_{jr}(X,t) g_{ks}(X,t+\tau)\, E[F_r(t)\, F_s(t+\tau)]d\tau \tag{55}$$

It is of interest to note that the right hand sides of (54) and (55) reduce to the same forms as those of (4) and (5), respectively, if the random excitations are delta-correlated.

If the right hand sides of the physical equations (1) are small in some sense, implying that the state variables are slowly varying, then the results obtained in (54) and (55) can be further simplified by time-averaging over t. This additional time averaging not only makes the drift and diffusion coefficients independent of time, but very frequently it also renders a group of state variables to become uncoupled from the others, thus permitting a reduction of the dimensions of the state space being considered. The latter advantage is very significant from an analytical point of view and is the main reason for the popularity of the stochastic averaging procedure. If the system is linear or slightly nonlinear, the unknowns in the original physical equations can be transformed to polar-coordinate variables corresponding to slowly varying amplitudes and phases, making the time-averaging applicable. Alternatively, the unknowns can be transformed to complex random processes in conjugate pairs. The

absolute magnitude of a complex random process is equivalent to an amplitude process, and the ratio between the imaginary and real parts is the arctangent of a phase process. This alternative scheme was used by Ariaratnam and Tam [38] to linear systems with many degrees of freedom. Brückner and Lin [39] have shown that it can also be applied advantageously to nonlinear cases, and when used in conjunction with the cumulant-neglect procedure, the number of equations to be solved simultaneously is reduced greatly.

Since time-averaging is often the key to make a problem solvable, it is of interest to comment on two cases for which time-averaging are still applicable without requiring that the right hand sides of all the first order physical equations be small. The first case is a weakly damped single-degree-of-freedom oscillator with a strongly nonlinear stiffness, governed by

$$\ddot{X} = - g(X) + \epsilon f(X,\dot{X}) + \epsilon^{1/2} h_j(X,\dot{X})F_j(t) \tag{56}$$

where ϵ is a small positive number and for simplicity the $F_j(t)$ are assumed to be white noises. Introduce an energy process [2]

$$V = \frac{1}{2}\dot{X}^2 + G(X) = \frac{1}{2}\dot{X}^2 + \int_0^X g(u)du \tag{57}$$

Equation (56) can be replaced by the following two first order equations

$$\dot{X} = \pm\sqrt{2(V - G)} \tag{58}$$

$$\dot{V} = \pm \sqrt{2(V-G)}\ \{\epsilon f(X,\pm \sqrt{2(V-G)}\ ) + \epsilon^{1/2}h_j(X,\pm\sqrt{2(V-G)}\ )F_j(t)\} \tag{59}$$

These two equations can be converted to the following Itô type equations

$$dX = \pm \sqrt{2(V-G)}\ dt \tag{60}$$

$$dV = \epsilon m dt + \epsilon^{1/2}\ \sigma\ dB(t) \tag{61}$$

where according to (4), (5), (45) and (46)

$$m = \pm \sqrt{2(V-G)}\ \{f + (\pi K_{jj})\ h_j\ \frac{\partial}{\partial V}[\pm \sqrt{2(V-G)}h_j]\} \tag{62}$$

$$\sigma = \sqrt{4\pi K_{ij}(V-G)h_i h_j} \tag{63}$$

The unknown V in (65) is slowly varying, but the unknown X in (60) is not. Invoking a theorem due to Khasminskii [40] Zhu [41] performed a time-averaging on the right-hand-side of (65) as follows:

$$\bar{m} = \frac{1}{T}\int_R \{f + \pi K_{ij}\, h_j \frac{\partial}{\partial V}[\pm\sqrt{2(V-G)}\, h_i]\}dX \tag{64}$$

$$\bar{\sigma}^2 = \pm\frac{1}{T}\int_R 2\pi K_{ij}\sqrt{2(V-G)}h_i h_j\, dX \tag{65}$$

where integration on t has been replaced by integration on X using (60), R is the integration domain defined as $V \geq G$, and

$$T = \pm\int_R [2(V-G)]^{-1/2}\, dX \tag{66}$$

Since the integrands are expressed in terms of $\pm\sqrt{2(V-G)}$, the value of each integral is obtained by adding the results from separate integrations for the plus and the minus signs. Substituting $\bar{m}$ and $\bar{\sigma}$ for m and σ, respectively, in (61), we obtain an Itô equation for V which is devoid of X. Similar analyses have also been carried out by Spanos [42] and Roberts [43] for systems under only additive random excitations.

Another exceptional case, considered by Namachchivaya and Lin [44], is described by the following equations of motion

$$\begin{aligned}\ddot{Z}_1 + 2\alpha_1\dot{Z}_1 + \Omega_1^2 Z_1 &= f_1(Z,\dot{Z},\mu) + A_{1j}(\mu)Z_j W(t)\\ \ddot{Z}_2 + 2\alpha_2\dot{Z}_2 + \Omega_2^2 Z_2 &= f_2(Z,\dot{Z},\mu) + A_{2j}(\mu)Z_j W(t)\end{aligned} \tag{67}$$

where μ is a parameter, $\Omega_i^2 = \omega_i^2(\mu) + \alpha_i^2(\mu)$, α_i and ω_i are damping parameters and natural frequencies, respectively, and f_i are only weakly nonlinear. As μ increases, the first mode becomes close to instability while the second mode remains highly damped. We then transform Z_1 and $\dot{Z}_1$ to the amplitude and phase counterparts, and at the same time make the substitution

$$Z_2 = [\cos\omega_2 t + \omega_2^{-1}\alpha_2 \sin\omega_2 t)Y_1 + (\omega_2^{-1}\sin\omega_2 t)Y_2]e^{-\alpha_2 t}$$

$$\dot{Z}_2 = [-(\omega_2^{-1}\Omega_2^2 \sin\omega_2 t)Y_1 + (\cos\omega_2 t - \omega_2^{-1}\alpha_2 \sin\omega_2 t)Y_2]e^{-\alpha_2 t} \qquad (68)$$

The new equations satisfy the condition for time averaging, and the resulting Itô equation for the amplitude of the first mode is devoid of other variables. This method was developed on the basis of a theorem due to Papanicolaou and Kohler [45]. It can be applied to cases involving a very large number of degrees of freedom. However, if more than one mode can become critical, then transformation to conjugate pairs of complex processes is simpler [46].

4 Energy Dissipation Balancing [47]

Consider a single-degree-of-freedom system, governed by equations of the type of (23). An exact stationary probability solution can be found if the ψ and θ functions are related according to (28). Restricting to $D(x_1) = 0$ and to λ of the form of (31), relation (28) is simplified to

$$\psi(x_1,x_2) = \pi x_2 K_{k\ell}\theta_k\theta_\ell\phi'(\lambda) - \pi K_{k\ell}\theta_i\frac{\partial}{\partial x_2}\theta_k + g(x_1) \qquad (69)$$

This equation specifies a class of solvable problems.

Given a problem with a ψ function not in the form of (69), it is possible to write

$$\psi(x_1,x_2) = u(x_1,x_2) + g(x_1) + \pi K_{k\ell}\theta_\ell \frac{\partial}{\partial x_2}\theta_k \qquad (70)$$

Then, using (12) as an approximate solution, the error involved is

$$\epsilon = u(x_1,x_2) - \pi x_2 K_{k\ell}\theta_k\theta_\ell\phi' + 2\pi K_{k\ell}\theta_\ell\frac{\partial}{\partial x_2}\theta_k \qquad (71)$$

A reasonable criterion for the choice of $\phi'(\lambda)$ is to equate the average energy dissipations between the given system and the substituting system [47] for which the exact solution is obtainable; namely letting

$$\int x_2\epsilon\, p_S(x_1,x_2)dx_1dx_2 = 0 \qquad (72)$$

where p_S is chosen to be the stationary probability density of the substituting system.

As an example, consider a van der Pol type oscillator

$$\ddot{Z} + \alpha\dot{Z} + \beta Z^2\dot{Z} + \gamma\dot{Z}^3 + Z + ZW_1(t) + \dot{Z}W_2(t) + W_3(t) \tag{73}$$

By equating $Z = X_1$ and $\dot{Z} = Z_2$ and comparing with (23), we can identify that $\theta_1 = x_1$, $\theta_2 = x_2$, $\theta_3 = 1$ and $\psi(x_1,x_2) = \alpha x_2 + \beta x_1^2 x_2 + \gamma x_2^3 + x_1$

$$\pi K_{k\ell}\theta_\ell \frac{\partial}{\partial x_2}\theta_k = \pi(K_{21}x_1 + K_{22}x_2 + K_{23}) \tag{74}$$

From (70),

$$\psi(x_1,x_2) = u(x_1,x_2) + g(x_1) + \pi(K_{21}x_1+K_{22}x_2+K_{23}) \tag{75}$$

Therefore,

$$\begin{aligned} g(x_1) &= x_1(1 - \pi K_{21}) - \pi K_{23} \\ u(x_1,x_2) &= (\alpha - \pi K_{22})x_2 + \beta x_1^2 x_2 + \gamma x_2^3 \end{aligned} \tag{76}$$

It follows from (31) that

$$\lambda = \frac{1}{2}x_2^2 + \frac{1}{2}(1 - \pi K_{21})(x_1 - x_{1,0})^2 \tag{77}$$

where $x_{1,0} = \pi K_{23}/(1 - \pi K_{21})$. In order for λ to be always positive, it requires that $1 - \pi K_{12} > 0$ which is a necessary condition in probability.

The integration in (72) can be simplified by a transformation $x_1 = [2\lambda/(1-\pi K_{21})]^{1/2}\cos\theta + x_{1,0}$, and $x_2 = (2\lambda)^{1/2}\sin\theta$, resulting in

$$\phi'(\lambda) = \frac{2(\alpha+\pi K_{22}) + (\beta + 3\gamma)\lambda}{2\pi(1-\pi K_{21})(K_{11}x_{1,0}+2K_{31}x_{1,0}+K_{33}) + \pi[K_{11}+3K_{22}(1-\pi K_{21}]\lambda} \tag{78}$$

The approximate stationary probability denisty is

$$p_S(x_1,x_2) = C \exp\left[-\int \phi'(\lambda)d\lambda\right] \tag{79}$$

The reader is referred to [47] for details.

It is of interest to note that if only the additive random excitations are present then the approximate probability density obtained on the basis of energy dissipation balancing coincides with that obtained from a least mean-square

error criterion proposed by Caughey [48]; however, the two results are different if multiplicative random excitations are present. In the latter case, the energy dissipation criterion leads to correct bifurcation and/or instability conditions in some known examples while the least mean-square error criterion or stochastic averaging [47,49] do not.

Concluding Remarks

The length limitation of this report does not permit a thorough review of all important advances which took place in recent years toward solving nonlinear random vibration problems. It is therefore appropriate to suggest additional materials for interested readers. The earlier review by Caughey [50] remains most authoriative for works prior to 1971. A large portion of a survey, entitled, "Methods of Stochastic Dynamics" is devoted to nonlinear stochastic systems. For the very useful analytical tools of equivalent linearization and stochastic averaging, [21] and [37] are again suggested.

References

1. E. WONG and M. ZAKAI 1965 Internal Journal of Engineering Scienes 4, 213-229. On the relation between ordinary and stochastic equations.

2. R. L. STRATONOVICH 1963 Topics in the Theory of Random Noise. Vol. 1. New York: Gordon annd Breach.

3. Y.K. LIN, Y. YONG and G.Q. CAI 1987 Stochastic Structural Mechanics. Lecture Notes in Engineering 31, 268-280. New York: Springer-Verlag. Exact solution for nonlinear systems under parametric and external white-noise excitations.

4. G.Q. CAI and Y.K. LIN 1988 Internal Journal of Nonlinear Mechanics. On exact stationary solutions of equivalent nonlinear stochastic systems. To appear.

5. R. GRAHAM and H. HAKEN 1971 Zeitschrift fur Physik, 203, 289-302. Generalized thermo-dynamic potential for Markow systems in detailed balance and far from thermal equilibrium.

6. Y. YONG and Y.K. LIN 1987 Journal of Applied Mechanics, 54, 414-418. Exact stationary-response solution for second order nonlinear systems under parametric and external white-noise excitations.

7. A. ANDRONOV, L. PONTRYAGIN and A. WITT 1940 Zh. Eksperim, i Teor. Fiz. 3, 165-180. On the statistical investigation of dynamical systems, in Russian.

8. A. KRAMERS 1940 Physica, 7, 284-304. Brownian motion in a field of force and diffusion model of chemical reactions.

9. T. K. CAUGHEY and F. MA 1983 International Journal of Nonlinear Mechanics, 17, 137-142. The exact steady-state solution of a class of nonlinear stochastic systems.

10. M. F. DIMENTBERG 1982 International Journal of Non-Linear Mechanics, 17, 231-236. An exact solution to a certain nonlinear random vibration problem.

11. Y.K. LIN and G.Q. CAI 1988 Journal of Applied Mechanics. Exact stationary-response solution for second order nonlinear systems under parametric and external white-noise excitations, Part II. To appear.

12. Y.K. LIN and G.Q. CAI 1988 Journal of Applied Mechanics. Equivalent stochastic systems. To appear.

13. M. SAN MIGUEL and S. CHATURVEDI 1980 Zeitschrift fur Physik B 40, 167-174. Limit cycles and detailed balance in Fokker-Planck equations.

14. W.F. WU and Y.K. LIN 1984 International Journal of Nonlinear Mechanics, 19, 349-362. Cumulant-neglect closure for nonlinear oscillators under random parametric and external excitations.

15. R.A. IBRAHIM, A. SOUNDARARAJAN and H. HEO 1985 Journal of Applied Mechanics, 52, 965-970. Stochastic response of nonlinear dynamics systems based on non-Gaussian closure.

16. Y. K. LIN 1986 Probabilistic Engineering Mechanics 1, 23-27. Some observations on stochastic averaging method.

17. K. ITÔ 1951 Nagoya Mathematical Journal, Japan 3, 55-65. On a formula concerning stochastic differentials.

18. Y.K. LIN 1967 Probabilistic Structural Dynamics. New York: McGraw-Hill (Reprinted with revision 1976: Krieger Publishing Co., Malabar, FL.)

19. S.T. ARIARATNAM 1980 In New Approaches to Nonlinear Problems in Dynamics, Ed. P.J. Holmes, SIAM Publications, Philadelphia, PA, 470-473. Bifurcation in nonlinear stochastic systems.

20. J.Q. SUN and C.S. HSU 1987 Journal of Applied Mechanics, 54, 649-655. Cumulent-Neglect Closure for Nonlinear Systems under Random Excitations.

21. P.D. SPANOS 1981 Applied Mechanics Reviews, 34, 1-8. Stochastic Linearization in Structural Dynamics.

22. S.A. ASSAF and L.D. ZIRKIE 1976 International Journal of Control, 23, 477-492. Approximate analysis of non-linear stochastic systems.

23. S.H. CRANDALL 1980 International Journal of Nonlinear Mechanics, 15, 303-313. Non-Gaussian closure for random vibration of non-linear oscillator.

24. A. BRUCKNER and Y.K. LIN 1987 International Journal of Nonlinear Mechanics, 22, 227-235. Generalization of the equivalent linearization method for nonlinear random vibration problems.

25. R.Z. ZHASMINSKI 1966 Theory of Probability and Applications. II(3), 390-405. A limit theorem for the solution of differential equations with random right hand sides.

26. G.C. PAPANICOLAOU and W. KOHLER 1974 Communication on Pure and Applied Mathematics, 27, 641-668. Asymptotic theory of mixing stochastic ordinary differential equations.

27. S.T. ARIARATNAM 1965 Proceedings, International Conference on the Dynamic Stability of Structures, 255-265. Oxford: Pergamon Press. Dynamic stability of a column under random loading.

28. Y.K. LIN, Y. FUJIMORI and S.T. ARIARATNAM 1979 AIAA Journal, 17, 545-552. Rotor blade stability in turbulent flow, Part I.

29. Y. FUJIMORI, Y.K. LIN and S.T. ARIARATNAM 1979 AIAA Journal, 17, 673-678. Rotorblade stability in turbulent flow, Part II.

30. J.E. PRUSSING and Y.K. LIN 1982 Journal of American Helicopter Society 27, 51-57. Rotor blade flap-lag stability in turbulent flow.

31. J.E. PRUSSING and Y.K. LIN 1983 Journal of American Helicopter Society 28, 42-46. A closed form analysis of rotor blade flap-lag stability in hover and low-speed forward flight in turbulent flow.

32. Y.K. LIN 1979 Journal of Engineering Mechanics, ASCE 105 EM6, 921-932. Motion of suspension bridges in turbulent winds.

33. C.G. BUCHER and Y.K. LIN 1988 Journal of Engineering Mechanics ASCE. Stochastic stability of bridges considering coupled modes. To appear.

34. N. SRI NAMACHCHIVAYA and S.T. ARIARATNAM 1987 International Journal of Nonlinear Mechanics 22, 363-372. Stochastically purburbed Hopf bifurcation.

35. N. SRI NAMACHCHIVAYA 1988 Journal of Applied Mechanics. Hopf bifurcation in the presence of both parametric and external stochastic excitations. To appear.

36. N. SRI NAMACHCHIVAYA 1988 Journal of Applied Mathematics and Computation. Stochastic bifurcations. To appear.

37. J.B. ROBERTS and P.D. SPANOS 1986 International Journal of Nonlinear Mechanics 21, 111-134. Stochastic averaging an approximate method of solving random vibration problems.

38. S.T. ARIARATNAM and D.S.F. TAM 1979 Z. Angew. Math. Mech. 59, 79-84. Random vibration and stability of a linear parametrically excited oscillators.

39. A. BRÜCKNER AND Y.K. LIN 1987 International Journal of Nonlinear Mechanics 22, 237-250. Applications of complex stochastic averaging to nonlinear random vibration problems.

40. R.Z. KHASMINSKII 1968 Kibernetika 4, 260-279. On the averaging principal for stochastic differential Itô equations (in Russian).

41. W.Q. ZHU 1982 Proceedings, IUTAM Symposium on Random Vibration and Reliability, Frankfurt/Oder, ed. K. Hennig, 347-357. Berlin: Akademie. Stochastic averaging of energy envelope of nearly Lyaponuv systems.

42. P.D. SPANOS 1982 Proceedings, IUTAM Symposium on Random Vibration and Reliability, Frankfurt/Oder, ed. K. Henning 327-337. Berlin: Akademie. Approximate analysis of random problems through stochastic averaging.

43. J.B. ROBERTS 1982 Proceedings, IUTAM Symposium on Random Vibration and Reliability, Frankfurt/Oder, ed. K. Hennig, 285-294. Berlin: Akademie. Energy methods for nonlinear systems with non-white excitation.

44. N. SRI NAMACHCHIVAYA and Y.K. LIN 1987 Stochastic Structural Mechanics. Lecture Notes in Engineering 31, 281-310. New York: Springer-Verlag. Application of stochastic averaging for systems with high damping.

45. G.C. PAPANICOLAOU and W. KOHLER 1976. Communications in Mathematical Physics, 46, 217-232. Asymptotic analysis of deterministic and stochastic equations with rapidly varying components.

46. C.G. BUCHER and Y.K. LIN 1988 Effect of spanwise correlation of turbulence field on the motion stability of long-span bridges. To appear.

47. G.Q. CAI and Y.K. LIN 1988 Internal Journal of Nonlinear Mechanics. A new approximate solution technique for randomly excited nonlinear oscillators. To appear.

48. T.K. CAUGHEY 1986 Journal of Probabilistic Mechanics 1, 2-4. On the response of nonlinear oscillators to stochastic excitation.

49. Y. K. LIN and G.Q. CAI 1988 Developments in Theoretical and Applied Mechanics 14. Energy dissipation balancing -- an approximate solution technique for nonlinearly damped system under random excitations. To appear.

50. T.K. CAUGHEY 1971 Advances in Applied Mechanics, II, 209-253. Nonlinear theory of random vibration.

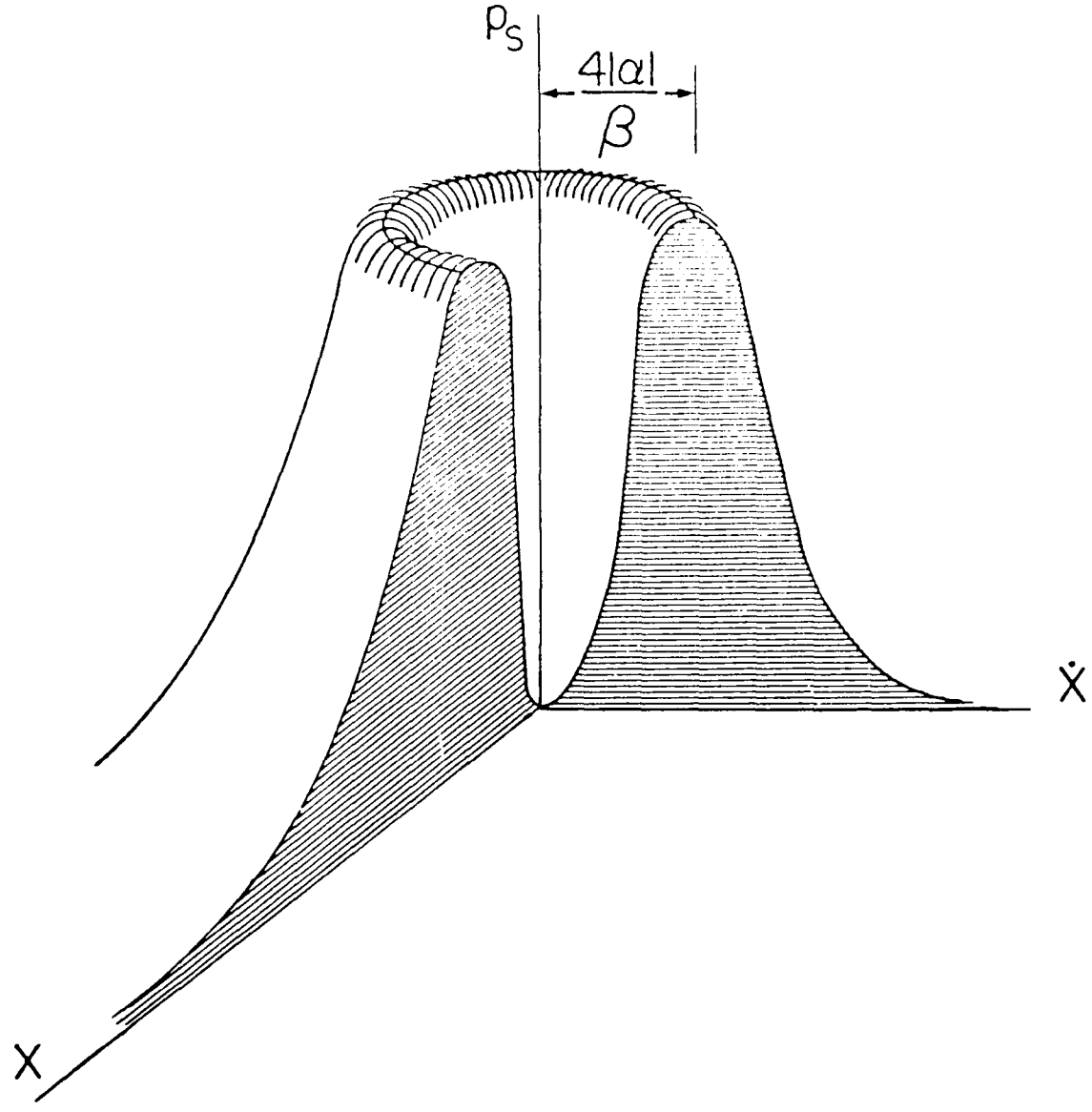

Fig. 1 A stationary probability density (with the right-front quarter removed), depicting the stochastic analogue of limiting-cycle behavior of a non-linear system under parametric excitation.

RESEARCH PERSONNEL

Principal Investigator: Y. K. Lin, Charles E. Schmidt Eminent Chair in Engineering and Director, Center for Applied Stochastics Research

Research Associate: Y. Yong, Assistant Professor, Center for Applied Stochastics Research and Ocean Engineering.

Research Assistant: G. Q. Cai, Center for Applied Stochastics Research.

Research Assistant: J.S. Wu, Center for Applied Stochastics Research

PUBLICATIONS GENERATED FROM THE RESEARCH PROJECT

The following technical articles have been generated from the present research project, with acknowledgement for AFOSR support:

(1) Y. Yong and Y. K. Lin, "Propagation of Decaying Waves in Periodic and Piece-Wise Periodic Structures," Journal of Sound and Vibration, Vol. 129, No. 2, 1989, pp. 99-118.

(2) Y. K. Lin, "Recent Advances in Nonlinear Random Vibration", AFWAL-TR-88-3034, 1988, Flight Dynamics Laboratory, Air Force Wright Aeronautical Laboratories, Wright-Patterson AFB, OH 45433, Vol. II, 1988, pp. 717-736.

(3) Y. K. Lin and G. Q. Cai, "Vibration of Nonlinear Systems under Additive and Multiplicative Random Excitations," Applied Mechanics Review, Vol. 42, No. 11, Part 2, Nov. 1989, pp. S135-141.

(4) Y. Yong and Y. K. Lin, "Dynamics of Complex Truss-Type Space Structures," Proceedings of AIAA/ASME/ASCE/AHS/ASC 30th Structures, Structural Dynamics and Materials (SDM) Conference, Mobile, AL, April 3-5, Part III, 1989, pp. 1295-1304.

(5) G. Q. Cai and Y. K. Lin, "Localization of Wave Propagation in Disordered Periodic Structures", accepted for publication in the AIAA Journal, also accepted for presentation at the AIAA/ASME/ASCE/ASC 31st Structures, Structural Dynamics and Materials Conference, Long Beach, CA April 2-4, 1990.

(6) Y. Yong and Y. K. Lin, "Wave Propagation in Truss-Type Structural Network", accepted for presentation at the AIAA/ASME/ASCE/AHS/ASC 31st Structures, Structural Dynamics and Materials Conference, Long Beach, CA, April 2-4, 1990.

(7) Y. Yong and Y.K. Lin, "Dynamic Response Analysis of Truss-Type Structural Networks," submitted for publication in the Journal of Sound and Vibration.

PROPOSED FUTURE RESEARCH

Continuation of the present research may proceed in several directions. We have investigated the localization effects due to random variabilities of material properties and manufacturing processes for disordered structural units with mono-coupling, which permits only one type of wave to propagate from cell to cell in the structure. It must be generalized to the case of multi-coupling, because the truss-type structural networks are capable of transmitting as many as 24 types of structural waves. The generalization is a major challenge, since multi-wave transmission permits re-composition or dispersion among different wave modes. The computation of the localization factor in the multi-wave case is analogous to the computation of the so-called largest Lyapunov exponent for a dynamical system defined in a large dimensional space, which is still an unsolved problem. In order to attempt a break-through, both analytical and simulation approaches may have to be employed.

Although we have developed several rather general schemes for obtaining exact and approximate solutions for randomly excited nonlinear structures. The application to aerospace structures have, by and large, been limited to single-degree-of-freedom systems. Recognizing the fact that idealized conditions for exactly solvable systems can seldom be met for multi-degree-of-freedom aerospace structures, approximate solutions are the norm rather than exceptions. However, the class of generalized stationary potential is too wide when applied to the case of multi-degree-of-freedom systems; and the accuracy of an approximate solution for this case on the basis of dissipation energy balancing may be questionable. It is, therefore, necessary to reduce the size of the class in order to obtain meaningful approximations.

Finally, a new stochastic structural control algorithm should be developed on the basis of controlling wave motions in disordered structures. This

approach is different from what has usually been used in the past in which emphasis is placed on controlling the response in various normal modes. We believe that the modal approach is inappropriate for large space structures exposed to essentially transient excitations, for which there is not sufficient time for the modal response to be generated fully. A wave propagation approach is more direct and more effective.